

Interlayer magnetic coupling in metallic multilayer structures

Zhu-Pei Shi* and Peter M. Levy

Department of Physics, New York University, 4 Washington Place, New York, New York 10003

John L. Fry

Physics Department, University of Texas at Arlington, Arlington, Texas 76019

(Received 18 November 1993)

The Anderson model of local state-conduction electron mixing is applied to the problem of interlayer magnetic coupling in metallic multilayered structures. Two types of coupling, Ruderman-Kittel-Kasuya-Yosida (RKKY) and superexchange arise from this interaction. The RKKY coupling comes only from intermediate states which correspond to spin excitations of the Fermi sea, that is, states corresponding to electron-hole pair production in the Fermi sea with an attendant spin flip. The superexchange coupling arises from virtual-charge excitations in which electrons from local states are promoted above the Fermi sea (one from each layer); this provides a second contribution to the coupling, that is in addition to the RKKY coupling. Moreover, the RKKY coupling is largely influenced by the topology of the Fermi surface and contains oscillatory modes of the coupling while superexchange coupling does not contain much Fermi-surface information. The RKKY coupling is ferromagnetically biased, while the superexchange coupling is antiferromagnetically biased. The total interlayer coupling (RKKY plus superexchange) resembles the oscillatory coupling of magnetic impurities in a free electron gas (the conventional RKKY coupling or Lindhard range function), but is antiferromagnetically biased if the density of states has a relatively large peak just above the Fermi energy. These characteristics are visible in two ways in experimental data: (i) the spin polarization pattern in the spacer layer between magnetic ones can be different from that of the interlayer magnetic coupling, and (ii) some metallic multilayered structures could have relatively large antiferromagnetic biases in their interlayer magnetic coupling; for example, Fe/Cr systems.

I. INTRODUCTION

In metallic systems, magnetic interactions are propagated by itinerant electrons and thus can be transmitted over relatively long distances. It follows that these interactions can couple magnetic layers through nonmagnetic metallic layers. Magnetic layers are usually Fe, Co, and Ni, but Ni is seldom picked up by experimentalists because of its small magnetic moment. Nonmagnetic spacers are either transition metals or noble metals. Interest in the interlayer magnetic coupling has been increased by the discovery of unexpected long-range oscillations in the variation of the coupling constant with the thickness of the spacer layers,¹ and a large number of systems have been investigated during the last years. Among the most striking results is the reporting of a multiperiodic oscillatory coupling for the Fe/Cr/Fe(001) system:²⁻⁴ The superposition of short-period 2 ML (ML denotes monolayer) and long-period 10–12 ML oscillations is observed. Similar results were also reported in Fe/Mn/Fe(001),⁵ Fe/Mo/Fe(001),⁶ and Co/Cu/Co(001).^{7,8} The explanation of this phenomenon is a challenge to the theory. The coupling interactions (order of strength 10^{-3} eV/magnetic moment pair) that are observed in the experiments are too large to be ascribed to magnetic dipolar interactions (order of strength 10^{-5} – 10^{-6} eV/magnetic moment pair); thus one has to consider some indirect coupling mechanisms. There are basically two strategies

that have been used theoretically to study the interlayer magnetic coupling: (i) total energy calculations and (ii) perturbative models.

The magnetic coupling could be determined by calculating the energy difference between corresponding multilayers having successive magnetic slabs ferromagnetically or antiferromagnetically aligned, all as a function of spacer thickness. There are three types of total energy calculations: (i) *ab initio* calculations,^{9,10} (ii) tight-binding calculations,¹¹⁻¹³ and (iii) a quantum well approach.¹⁴⁻¹⁸ The first two are quite difficult because the energy difference is several orders of magnitude smaller than the total energy itself. To obtain the numerical accuracy necessary to discern the small differences in energy, total energy calculations have been restricted to relatively small spacer layer thicknesses, and appear not well suited for investigating long-period oscillatory coupling. From these calculations, it seems difficult to gain a simple intuitive picture of the physical mechanism involved in the coupling phenomenon. A one-dimensional quantum well may be the simplest model to illustrate the interlayer magnetic coupling. The specific calculation in terms of matching free electron wave functions in a quantum well is exhibited by Barnas¹⁴ and by Erickson, Hathaway, and Cullen¹⁵⁻¹⁷ for the cases of ferromagnetic and antiferromagnetic alignments. In the latter calculation the coupling is determined from the torque acting on the spin current as a function of energy. This is in appar-

ent contrast with the calculation performed by Stiles,¹⁸ which is done in terms of a change in density of states as a function of energy. In fact, their calculations are formally identical, and give the same result. In these calculations, the band structures of the magnetic and spacer layers are treated in a free electron gas approximation (an isotropic s band), and the reflection probabilities are determined by matching free electron wave functions at the interfaces between the materials. Calculated transition-metal band structures indicate that the d band is narrower and has a higher density of states than the free-electron-like contribution of the s band alone.¹⁹ It seems that this quantum well model, i.e., a Krönig-Penney potential for metallic superlattices, is an oversimplified band structure model to mimic a situation of magnetic multilayered structures with transition-metal spacers because one is ignoring features of the d bands.

In view of the difficulties with total energy calculations, it is tempting to attack the problem of interlayer magnetic coupling in a different way, and to attempt to obtain the coupling directly, without having to compute the total energy. Even though total energy calculations are undoubtedly needed to obtain the strength of the interlayer magnetic coupling, perturbative methods provide greater insight into the origin of this coupling. Invariably, in a perturbative approach, one has to make approximations that are usually suggested *a priori* by physical intuition.

The oscillatory behavior of interlayer coupling in noble-metal systems bears much resemblance to the one observed for the Ruderman-Kittel-Kasuya-Yosida (RKKY) interaction between magnetic impurities.^{20–22} Thus the RKKY interaction appears a good candidate for the mechanism of oscillatory interlayer magnetic coupling. Bruno and Chappert²³ have extended the analysis of Roth, Zeiger, and Kaplan²⁴ on the RKKY coupling between spins for nonspherical Fermi surfaces to the coupling between two sheets of spins. They focus on the topology of the Fermi surfaces, e.g., nesting features, to successfully predict periods of the oscillations observed in the interlayer magnetic coupling in noble-metal systems.

The RKKY theory of interlayer magnetic coupling relies on the assumption that the ferromagnetic layers can be described as two-dimensional arrays of localized spins, which interact with the conduction electrons of the spacer material via a structureless contact potential. In the case of ferromagnetic-nonmagnetic transition-metal layered structures this approximation is very crude and cannot correctly predict either the strength of the coupling or the phase of the oscillations. In order to be able to improve upon this one needs a better description of the interaction between the ferromagnetic layer and the conduction electrons of the spacer.

Wang, Levy, and Fry²⁵ used the s - d mixing interaction and paramagnetic band structure for chromium to calculate the interlayer magnetic coupling in an Fe/Cr/Fe(001) multilayered structure. They obtained a 10 ML long-range oscillation, in agreement with experimental results known at that time,¹ and predicted a 2 ML rapid oscillation. They showed that the 2 ML oscillation is readily suppressed by interfacial roughness, explaining why it had not been seen. Using superlattices with sharper

interface this theoretical prediction 2 ML oscillation was verified experimentally by Unguris *et al.*² and Demokritov *et al.*⁴

In spite of the success of these perturbative methods in explaining the coupling between magnetic impurities in transition-metal alloys, one might be skeptical about the results of a perturbative calculation of the coupling between two sheets of spins, especially when the spacer layer has a propensity to be magnetic. Deaven *et al.*²⁶ considered a tight-binding model of a quasi-one-dimensional magnetic multilayer with one orbital per site and with hopping and exchange interactions between sites. They solved for the spin configurations by iterating their solutions until they were self-consistent. The energy difference between the ferro- and antiferromagnetic configurations yields the interlayer magnetic coupling. In their model, this coupling comes from the hybridization (mixing) of magnetic and nonmagnetic states at interfaces. They compared their solution with RKKY theory and concluded that perturbation theory is sufficient to understand the *qualitative* features of this fully interacting model system, e.g., of the coupling in the asymptotic limit of large spacer layer thickness.

Recently, we applied the Anderson model of the local-state-conduction-electron mixing interaction to the problem of interlayer magnetic coupling again and presented two types of excitation mechanisms: low-energy spin excitations, which give rise to RKKY coupling [$J_{\text{RKKY}}(z)$], and high-energy charge excitations, which produce superexchange coupling [$J_S(z)$]. We interpreted successfully²⁷ the coupling in Fe/Cr/Fe multilayered structures, and expect that this model may also work for noble-metal spacer layers.

In this paper we focus on perturbative methods, and consider the interlayer magnetic coupling coming from spin scattering of itinerant electrons. We will consider two sources of scattering: the Coulomb exchange interaction and the mixing interaction, and in following sections we will develop the spin polarization and interlayer magnetic coupling coming from these two distinct sources. The organization of the paper is the following: In Sec. II we discuss spin polarization and RKKY coupling. We present two types of excitations based on the Anderson model to discuss the RKKY coupling and an additional purely antiferromagnetic coupling (superexchange) in Sec. III. In Sec. IV we derive the interlayer magnetic coupling in the free electron gas approximation, which may be suitable for noble metals. Interlayer magnetic coupling in transition-metal systems is studied in Sec. V, and in Sec. VI we summarize our results.

II. SPIN POLARIZATION AND RKKY COUPLING

Many of the models proposed for interlayer magnetic coupling between two ferromagnetic layers through a paramagnetic layer follow from earlier work on the coupling between magnetic impurities in a host metal. This is the Ruderman-Kittel-Kasuya-Yosida (RKKY) coupling, first proposed for nuclear spins, but later applied to both transition metals with magnetic impurities and

to the localized f -electron coupling in rare earth metals.

The RKKY interaction was derived by Ruderman and Kittel²⁰ for the indirect coupling of two nuclear spins via their hyperfine contact interaction with the conduction electrons. They proposed a contact potential of the form

$$V(\mathbf{r}, \mathbf{s}) = A\delta(\mathbf{r} - \mathbf{R}) \mathbf{s} \cdot \mathbf{S} \quad (1)$$

for the interaction between the spin \mathbf{S} at site \mathbf{R} and the spin of a conduction electron \mathbf{s} at position \mathbf{r} . This form was extended later by Kasuya²¹ and Yosida²² who proposed a similar coupling between localized d or f electrons and the conduction electrons.

The essence of this interaction is that one magnetic impurity interacts with the conduction electrons of a host metal and induces a spin polarization in the electron gas. This spin polarization extends throughout the host metal and eventually reaches a second magnetic impurity, thus giving rise to an effective interaction between the two given magnetic impurities. In the limit of large separation (r) between these two impurities, when the host metal is treated as an uniform electron gas, the coupling oscillates periodically with an oscillation period (π/k_F) related to the diameter of the *spherical* Fermi surface with an amplitude decaying like $1/r^3$. For a nonspherical Fermi surface in a real metal the oscillation periods are determined by the topology of the Fermi surface, i.e., extremal wave vectors spanning the Fermi surface.²⁴

The first extension of the RKKY model to the case of two interacting magnetic layers was done by Yafet,²⁸ to explain the coherence of magnetization of Gd layers separated by nonmagnetic Y layers in Gd/Y superlattices. He treated the Gd layers as localized spins and used the computed wave-vector-dependent susceptibilities of Gd and Y (Ref. 29) to obtain an effective Gd-Y q -dependent exchange interaction. The resulting interlayer magnetic coupling, $J(z)$, is obtained by taking the one-dimensional Fourier transform of the effective q -dependent exchange interaction. The resulting $J(z)$ shows a well-defined oscillation for Y thickness z between 4 and 11 ML. For large z , irregular oscillations reflect the structure of the susceptibility $\chi(q)$, with interference occurring between many wave vectors with roughly equal contributions to the susceptibility. Yafet³⁰ pointed out that the RKKY range function of a single ferromagnetic layer in three-dimensional space (a pseudo-one-dimensional system) falls off asymptotically as $1/z^2$, where z is a distance away from the layer. Baltensperger and Helman³¹ also calculated the coupling of ferromagnets separated by a nonmagnetic layer; they found the RKKY theory gives an expression in which the coupling oscillates as a function of the thickness of the nonmagnetic layer, and asymptotically decreases as the reciprocal square of the thickness. Their expressions indicate that the coupling also depends on thickness of the magnetic layer, but recent experimental data³² show that the

coupling does not strongly depend on the thickness of the magnetic layer. Magnetic ordering in rare earth superlattices was also considered by Fairbairn and Yip³³ who calculated the RKKY coupling using wave functions computed for a superlattice of square well potentials.

Oscillations in the interlayer magnetic coupling observed for magnetic-nonmagnetic transition-metal metallic multilayered structures suggested that the RKKY model might be applied to those materials as well. For magnetic multilayers with noble-metal spacer layers, Bruno and Chappert²³ took the RKKY range function to describe the interaction between every pair of spins in a layered structure, and calculated an interlayer magnetic coupling energy by simply summing these interactions. They focused on the Fermi surface and predicted all possible oscillations for noble-metal spacer layers; their results are in excellent agreement with experimental data.⁷

In this section the application of RKKY coupling to magnetic multilayers with transition-metal spacers, especially Cr, is discussed. We find in this case that the RKKY coupling alone is not enough to interpret the experimental data.

A. Spin polarization

We consider a system of conduction electrons in a metal that is spin polarized by the presence of a local magnetic moment at site \mathbf{R} . This polarization effect is attributed to a coupling between the local moment and conduction electron Bloch states $n_1\mathbf{k}$ and $n_2\mathbf{k}'$ of the form³⁴

$$H = - \sum_{n_1\mathbf{k}, n_2\mathbf{k}'} I_{n_1\mathbf{k}, n_2\mathbf{k}'}(\mathbf{R}) (\Psi_{n_1\mathbf{k}}^\dagger \mathbf{s} \Psi_{n_2\mathbf{k}'})(\Psi_{n_2\mathbf{k}'}^\dagger \mathbf{S} \Psi_{n_1\mathbf{k}}) \quad , \quad (2)$$

where $I_{n_1\mathbf{k}, n_2\mathbf{k}'}$ is a slowly varying well-behaved function of \mathbf{k} and \mathbf{k}' , whose specifications depend upon the particular mechanism which produces the scattering. The first-order correction to the Bloch functions due to a magnetic ion is given as

$$\psi_{n_1\mathbf{k}, \pm} = \psi_{n_1\mathbf{k}, \pm}^0 \pm \frac{S}{2} \sum_{n_2\mathbf{k}'} \frac{I_{n_1\mathbf{k}, n_2\mathbf{k}'}(\mathbf{R})}{\varepsilon_{n_2\mathbf{k}'} - \varepsilon_{n_1\mathbf{k}}} \psi_{n_2\mathbf{k}', \pm}^0 \quad , \quad (3)$$

where $\psi_{n\mathbf{k}, \pm}^0 = \phi_{n\mathbf{k}}(\mathbf{r})\chi_{\pm}$, $\phi_{n\mathbf{k}}(\mathbf{r})$ is the unperturbed spatial wave function and χ_{\pm} are the eigenstates of spin parallel and antiparallel to the local magnetic moment $\mathbf{S}(\mathbf{R})$, e.g., the magnitude is $S = 2.2\mu_B$ for iron (μ_B denotes Bohr magneton). With this, one finds that the spin polarization induced at a point \mathbf{r} by an impurity at the origin $\mathbf{R} = \mathbf{O}$ is

$$m(\mathbf{r}) = \langle s(\mathbf{r}) \rangle = S \sum_{n_1\mathbf{k}, n_2\mathbf{k}'} \left[I_{n_1\mathbf{k}, n_2\mathbf{k}'}(\mathbf{O}) \frac{f_{n_1\mathbf{k}}(1 - f_{n_2\mathbf{k}'})}{\varepsilon_{n_2\mathbf{k}'} - \varepsilon_{n_1\mathbf{k}}} \phi_{n_2\mathbf{k}'}^*(\mathbf{r}) \phi_{n_1\mathbf{k}}(\mathbf{r}) + \text{c.c.} \right] \quad , \quad (4)$$

where $f_{n\mathbf{k}}$ is the Fermi distribution function. In reciprocal space and at zero temperature, this can be written as

$$m(\mathbf{q}) = S \sum_{n_1, n_2, \mathbf{k}} \left[I_{n_1 \mathbf{k}, n_2 \mathbf{k}'}(O) M_{n_1 \mathbf{k}, n_2 \mathbf{k}'}(\mathbf{q}) \frac{\theta(\varepsilon_F - \varepsilon_{n_1 \mathbf{k}}) \theta(\varepsilon_{n_2 \mathbf{k}'} - \varepsilon_F)}{\varepsilon_{n_2 \mathbf{k}'} - \varepsilon_{n_1 \mathbf{k}}} + \text{c.c.} \right], \quad (5)$$

where θ is a step function, ε_F is the Fermi energy, $\mathbf{k}' = \mathbf{k} + \mathbf{q} + \mathbf{G}$, \mathbf{G} is a vector of the reciprocal lattice, and $M_{n_1 \mathbf{k}, n_2 \mathbf{k}'}(\mathbf{q}) \equiv \langle n_2 \mathbf{k}' | e^{-i\mathbf{q} \cdot \mathbf{r}} | n_1 \mathbf{k} \rangle$ is an atomic form factor matrix element.³⁵ This spin polarization can also be derived from a one-impurity Anderson model.³⁶

As the interaction strength between a local moment and conduction electrons is determined by the Bloch

states $n_1 \mathbf{k}, n_2 \mathbf{k}'$, one expects $I_{n_1 \mathbf{k}, n_2 \mathbf{k}'}$ to contain the form factor matrix element. Therefore if we write $I_{n_1 \mathbf{k}, n_2 \mathbf{k}'}(O) = A(\mathbf{q}) M_{n_1 \mathbf{k}, n_2 \mathbf{k}'}^*(\mathbf{q})$ for all \mathbf{k} , then Eq. (5) reduces to

$$m(\mathbf{q}) = S A(\mathbf{q}) \chi(\mathbf{q}), \quad (6)$$

where $\chi(q)$ is the random phase approximation (RPA) susceptibility written as³⁷

$$\chi(\mathbf{q}) = \sum_{n_1 \mathbf{k}, n_2} \frac{|M_{n_1 \mathbf{k}, n_2 \mathbf{k}'}(\mathbf{q})|^2 \theta(\varepsilon_F - \varepsilon_{n_1 \mathbf{k}}) \theta(\varepsilon_{n_2 \mathbf{k}'} - \varepsilon_F)}{\varepsilon_{n_2 \mathbf{k}'} - \varepsilon_{n_1 \mathbf{k}}}. \quad (7)$$

When one makes the free electron gas approximation $M_{n_1 \mathbf{k}, n_2 \mathbf{k}'}(\mathbf{q}) = 1$ the susceptibility reduces to

$$\chi(\mathbf{q}) = \sum_{\mathbf{k}} \frac{\theta(\varepsilon_F - \varepsilon_{\mathbf{k}}) \theta(\varepsilon_{\mathbf{k} + \mathbf{q}} - \varepsilon_F)}{\varepsilon_{\mathbf{k} + \mathbf{q}} - \varepsilon_{\mathbf{k}}}, \quad (8)$$

which yields the Lindhard function. In linear response theory, $m(\mathbf{q}) = \chi(\mathbf{q}) h(\mathbf{q})$; therefore from Eq. (6) one sees that $h(\mathbf{q}) = A(\mathbf{q}) S$, i.e., that the interaction with the local moment is equivalent to an external field acting on the conduction electrons.

Until now we have considered one local moment in a sea of conduction electrons. We model a magnetic layer as a sheet of spins which represent the interface immersed in the electron sea. For a *sheet* of local moments one must add the individual contributions from each moment, Eq. (4). *Equivalently* Yafet³⁰ has shown that the spin polarization induced at a distance z normal to a *sheet* of spins is the *one-dimensional* Fourier transform of Eq. (5), i.e.,

$$\langle m(z) \rangle_P = \frac{a}{2\pi} \int_0^\infty f(q_z) m(q_z) \cos(q_z z) dq_z, \quad (9)$$

where a is the repeat distance in the z direction, and $f(q_z)$ represents the roughness of the interface between the ferromagnetic substrate and the nonmagnetic overlayer. Here we approximate $f(q_z)$ by

$$f(q_z) = (1 - 2p) + 2p \cos\left(q_z \frac{a}{2}\right), \quad (10)$$

where p is an interface roughness parameter,²⁵ and the brackets around $m(z)$ denote the average taken by the roughness factor Eq. (10). In Sec. V [see Eqs. (36) and (37)], we discuss why it is appropriate to use the bracket notation.

B. RKKY coupling

The RKKY coupling between a spin polarization induced by one magnetic ion at origin O and another one at site \mathbf{r} is found by applying Eq. (2) and Eq. (3) to different sites of magnetic ions; the ensuing coupling is

$$J_{\text{RKKY}}(\mathbf{r}) = \sum_{n_1 \mathbf{k}, n_2 \mathbf{k}'} \left[I_{n_1 \mathbf{k}, n_2 \mathbf{k}'}(O) I_{n_1 \mathbf{k}, n_2 \mathbf{k}'}^*(\mathbf{r}) \frac{f_{n_1 \mathbf{k}}(1 - f_{n_2 \mathbf{k}'})}{\varepsilon_{n_2 \mathbf{k}'} - \varepsilon_{n_1 \mathbf{k}}} + \text{c.c.} \right], \quad (11)$$

where $I_{n_1 \mathbf{k}, n_2 \mathbf{k}'}^*(\mathbf{r}) = e^{i(\mathbf{k}' - \mathbf{k}) \cdot \mathbf{r}} I_{n_1 \mathbf{k}, n_2 \mathbf{k}'}(O)$. Equation (11) can also be expressed in reciprocal space at zero temperature as

$$j_{\text{RKKY}}(\mathbf{q}) = \sum_{n_1, n_2, \mathbf{k}} \left[\frac{|I_{n_1 \mathbf{k}, n_2 \mathbf{k}'}(O)|^2 \theta(\varepsilon_f - \varepsilon_{n_1 \mathbf{k}}) \theta(\varepsilon_{n_2 \mathbf{k}'} - \varepsilon_f)}{\varepsilon_{n_2 \mathbf{k}'} - \varepsilon_{n_1 \mathbf{k}}} + \text{c.c.} \right]. \quad (12)$$

According to Yafet's argument,³⁰ the RKKY coupling between two *sheets* of spins can be obtained directly by Fourier transforming Eq. (12), and is given as

$$\langle J_{\text{RKKY}}(z) \rangle_P = \frac{a}{2\pi} \int_0^\infty dq_z f_1(q_z) f_2(q_z) j_{\text{RKKY}}(q_z) \cos(q_z z), \quad (13)$$

where $f_1(q_z)$ represents the roughness of the interface between the ferromagnetic substrate and the nonmagnetic layer, and $f_2(q_z)$ represents the interface roughness between the magnetic *overlayer* and the nonmagnetic layer. The roughness at the interfaces we have considered is that part which represents uncorrelated fluctuations of the interfaces.²³ In Sec. V [see Eqs. (36) and (37)], we discuss the notation $\langle J(z) \rangle_p$.

If $I_{n_1 k, n_2 k'}(O) = A(\mathbf{q}) M_{n_1 k, n_2 k'}^*(\mathbf{q})$ for all \mathbf{k} , then the RKKY coupling, Eq. (12), is proportional to the susceptibility, i.e.,

$$J_{\text{RKKY}}(\mathbf{q}) = |A(\mathbf{q})|^2 \chi(\mathbf{q}) . \quad (14)$$

Yafet²⁸ used this form to study the interlayer magnetic coupling in Gd-Y superlattices and obtained results in agreement with experiments. A constant $A(\mathbf{q})$ in Eq. (14) has been employed by Bruno and Chappert²³ to study magnetic layers interacting through noble-metal spacers. They explained both the long-period oscillatory coupling and the multiperiodic oscillations in multilayered structures with noble-metal spacer layers, in terms of the topological properties of the spacer layer's Fermi surface.

The RKKY interlayer magnetic coupling can then be understood as occurring in three stages: the spin polarization of the conduction electrons of the host materials induced by one magnetic layer, the subsequent propagation of this spin polarization across the spacer layer, and finally the interaction of the spin-polarized electron gas with another magnetic layer.

Generally, the spin-dependent scattering of conduction electrons by the magnetic moments at the interfaces comes from two sources: the Coulomb exchange interaction and the mixing interaction. When the Coulomb exchange interaction dominates, the phenomenological interaction of conduction electrons with a magnetic moment can be described by Eq. (2), and $I_{n_1 k, n_2 k'}$ is often taken as a constant. On the other hand, for 3d transition metals the mixing interaction is much larger and dominates the Coulomb exchange interaction. For the magnetic multilayered structures with transition-metal spacer layers, we specifically considered that it is the *s-d mixing* interaction³⁸ rather than the local-electron-conduction-electron *exchange* interaction that gives the main contribution to $I_{n_1 k, n_2 k'}$. For the mixing interaction at the site O , this coupling is given by the one-site Schrieffer-Wolff transformation³⁹ as follows:

$$I_{n_1 k, n_2 k'}(O) = \frac{V_{n_2 k'}^* V_{n_1 k}}{\varepsilon_{n_2 k'} - \varepsilon_+} , \quad (15)$$

where ε_+ is the energy of the local impurity state relative to the bottom of conduction electron bands and $V_{n k}$ represents the strength of the mixing interaction.³⁸ The mixing interaction leads to a broadening or virtual bound state (VBS) description of local impurity levels in metals;⁴⁰ this introduces complex energy levels ε_+ in Eq. (15).

C. Spin polarization in Fe/Cr bilayers

The layer-by-layer spin polarization in epitaxial Cr on Fe(001) substrates has been observed below⁴¹ and well

above⁴² the bulk Cr Néel temperature T_N . These direct observations are notable achievements; the existence of polarization of the form of a spin density wave (SDW) in Cr for temperatures up to $1.8T_N$ deserves special attention. Below T_N it might be assumed that the SDW is spontaneous, with its wave vector possibly modified by epitaxial strain, and its amplitude a function of temperature (as it is in the bulk). The appearance of a SDW-like polarization above T_N may be explained as an enhanced T_N due to the presence of the Fe substrate, or it may be simply a polarization wave *induced* by the Fe substrate. Since experiments suggest that the SDW has a decaying amplitude as a function of the distance from the Fe substrate,⁴² we adopt the latter point of view here and present a calculation of the magnetization of paramagnetic Cr layers on an Fe(001) substrate.³⁶

To calculate the spin polarization in a Cr layer induced by an Fe substrate, we specifically use the paramagnetic chromium band structure. In Eq. (15), we set $\text{Re}[\varepsilon_+] = \varepsilon_F - E_h$, where E_h is the energy required to promote an electron from an occupied local magnetic impurity level to the Fermi level. Away from the interface, the induced spin polarization is essentially given by the susceptibility $\chi(\mathbf{q})$, i.e., $m(\mathbf{q}) \sim \chi(\mathbf{q})$. Therefore, for small \mathbf{q} , it is possible to make the ansatz $V_{n_1 k} V_{n_2 k'}^* = V^2 M_{n_1 k, n_2 k'}^*(\mathbf{q})$ in Eq. (15), which will be discussed in the Appendix. The d parts of the atomic form factors decrease rapidly with \mathbf{q} . Therefore in our calculations, the s and p parts of the atomic form factors are taken to be constants^{27,36} (being equivalent to an ansatz $V_{n_1 k} V_{n_2 k'}^* = \text{const}$ for large \mathbf{q}) so as to reflect the local or point-contact-like property of the *s-d* mixing.

With these approximations, we have calculated the spin polarization $m(q_z)$, Eq. (9), with $E_h = 0.08$ Ry and $\text{Im}[\varepsilon_+] = \Delta = 0, 0.04, 0.08, 0.16$ Ry. By taking $E_h = 0.08$ Ry we find the best fit to the experimental data on Fe/Cr/Fe(001) systems.²⁵ We plot only data for $\Delta = 0$ in Fig. 1. We have used the band structure that has been found to reproduce the incommensurate SDW instability occurring at $q_{\text{SDW}} \simeq 0.958\Gamma H$ in Cr.³⁷

In bulk chromium the moment of the SDW varies as

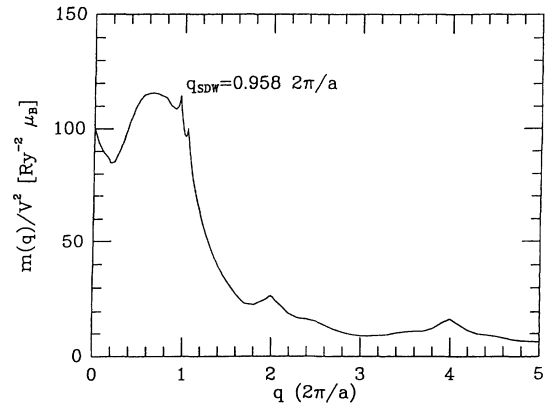


FIG. 1. The spin polarization $m(q)$ in Cr on Fe(001) calculated with $E_h = 0.08$ Ry. The twin peaks represent spin density wave ordering at $q_{\text{SDW}} = 0.958(2\pi/a)$ and $1.042(2\pi/a)$. V is expressed in rydbergs.

$\mu = \mu_b \cos(q_{\text{SDW}} z)$, where at zero temperature $\mu_b = 0.62\mu_B$. The period is given by $2\pi/q_{\text{SDW}}$, where $q_{\text{SDW}} = (\pi/d)(1 - \delta)$, d is the layer spacing, which is $a/2$ for the bcc lattice in the (001) direction, and δ is a measure of the incommensurability.⁴⁴ Here, the spin polarization $m(z)$ in a chromium overlayer is obtained by using the Fourier transform $m(z)$ [Eq. (9)] of $m(q)$ [Eq. (5)]. We find that a decaying SDW induced by the mixing interaction at an Fe/Cr interface gives rise to 2 ML oscillations with an envelope of 24 ML wavelength (being equivalent to $1/\delta$ with $\delta = 0.042$) and a long 10 ML period spin polarization which exist even for a rough interface ($p = 0.25$). In Fig. 2, we show our results for a smooth ($p = 0$), an irregular (not very rough, $p = 1/8$), and a rough ($p = 1/4$) interface for $E_h = 0.08$ Ry and $\Delta = 0$, i.e., for a narrow VBS. On comparing these with the recent data^{41,42} we find a reasonable resemblance. As the present calculation has not introduced the exchange enhancement in paramagnetic chromium, it is not realistic to compare the magnitude of this predicted induced spin polarization with the experimental data.

The main differences between our results and the data are that (1) nodes (phase slips in the language of Ref. 42) occur at $nl_S/2$ ($n = 1, 3, 5, \dots$), where l_S is the distance between nodes; we find that $l_S = 24$ ML, whereas experimentally it has been found that $l_S = 20$ ML (Ref. 42); (2) we find that the first node occurs in the region around 11–12 ML; this is consistent with the *apparent* phase slip at 10–11 ML observed by Walker *et al.*,⁴¹ but it does not agree with the first phase slip observed at 4–5 ML by Unguris *et al.*⁴²

The discrepancy in l_S probably comes from the strain in the chromium overlayer.⁴⁴ The virtual bound state *may* generate an additional phase^{45,46} so that the induced SDW would have the form $\mu_{\text{SDW}} \sim \mu_0(z)\cos(q_{\text{SDW}}z + \varphi_0)$, with a nonzero initial phase φ_0 , and $\mu_0(z)$ is a slowly decaying function. If one chooses

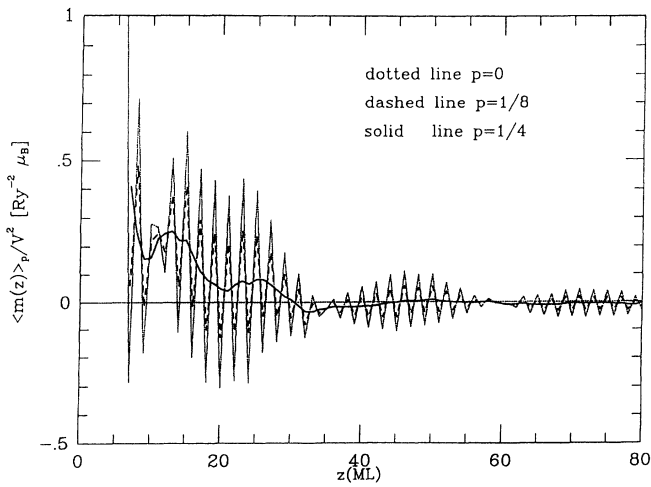


FIG. 2. The spin polarization $\langle m(z) \rangle_p$ in Cr on Fe(001) calculated with $E_h = 0.08$ Ry. The dotted line is for a smooth ($p = 0$) interface, the dashed line for an irregular one ($p = 1/8$), and solid line for rough interface ($p = 1/4$). V is expressed in rydbergs.

$\varphi_0(q_{\text{SDW}}) = \pi/3$ the phase slip regions are shifted and occur around 4, 24, 44, and 64 ML, etc., for $q_{\text{SDW}} = 0.95\Gamma H$ (being equivalent of $l_S = 20$ ML); this is exactly what has been experimentally observed⁴² in one of the two experiments. However, the $m(q)$ we find for a paramagnetic chromium layer is not simply $m(q_{\text{SDW}})\delta(q - q_{\text{SDW}})$; rather it contains a spectrum of q vectors, as shown in Fig. 1. To allow for the complex energy entering $m(\mathbf{q})$, $m(q_z)$ is complex and expressed as $|m(q_z)| e^{i\varphi(q_z)}$, and then we generalize Eq. (9) as follows:

$$\langle m(z) \rangle_p = \frac{a}{2\pi} \int_0^\infty f(q_z) |m(q_z)| \cos[q_z z + \varphi(q_z)] dq_z, \quad (16)$$

where $|m(q_z)| = \sqrt{\{\text{Re}[m(q_z)]\}^2 + \{\text{Im}[m(q_z)]\}^2}$, and $\varphi(q_z) = \tan^{-1}\{\text{Im}[m(q_z)]/\text{Re}[m(q_z)]\}$. In Fig. 3, we plot the spin polarization $m(z)$ with $\Delta = 0.04, 0.08, 0.16$ Ry, and do *not* find much shifting in the nodes or phase slip regions. Rather we find that the main effects of the finite width of the VBS are (1) an attenuation of the amplitude of the induced oscillation of the spin density and (2) a decrease in the ferromagnetic bias in the induced magnetization for z less than 15 ML. Therefore we conclude that for chromium the finite width of the iron VBS does not produce discernible effects such as phase shifts

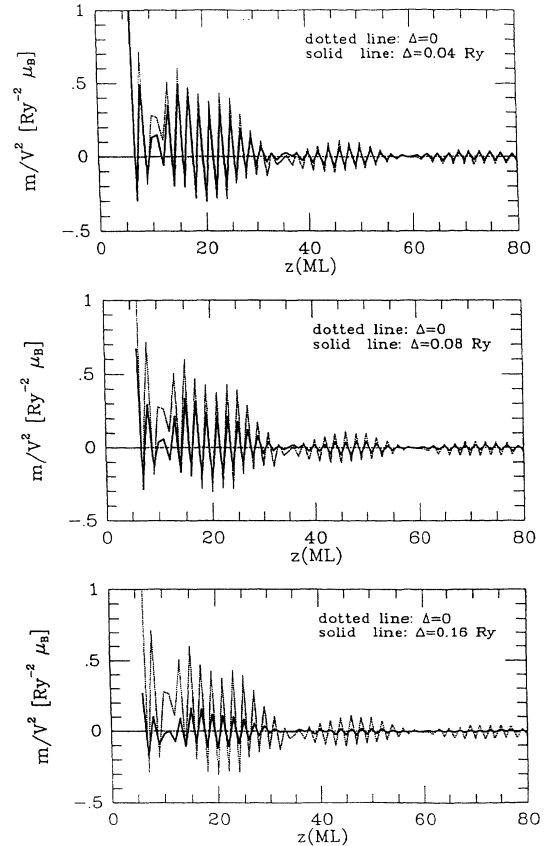


FIG. 3. Comparison of spin polarization for local state with no broadening and a VBS with $\Delta = 0.04, 0.08$, and 0.16 Ry for $E_h = 0.08$ Ry and a smooth interface ($p = 0$).

in the asymptotic region (large z); rather its effects are limited to the *preasymptotic* region.

In summary, we have derived the spin polarization in a paramagnetic layer induced by the mixing interaction between local and conduction electrons at the interface of a magnetic-paramagnetic bilayer system. We have included the effects of the imaginary part of the self-energy of the local state on the induced spin polarization. Based on the band structure of bulk paramagnetic chromium, our theoretical spin polarization pattern resembles the experimental data. The effects of the finite width of the VBS are seen at short distances (small thicknesses of chromium layer), but do not show up in the asymptotic region. When one puts another magnetic layer over the chromium, one picks up the interaction between this induced spin polarization and the magnetic overlayer, and it gives an RKKY-like interlayer magnetic coupling.

D. RKKY coupling in Fe/Cr multilayered structures

We have calculated the $J_{\text{RKKY}}(z)$ coupling by using the same parameters as for the induced spin polarization; our results are shown in Fig. 4(a) for $p_1 = p_2 = 0$, $1/8$, and $1/4$, where we have assumed, lacking more precise information, that both interfaces are equally rough (smooth). This coupling with a strong ferromagnetic bias does *not* resemble the interlayer magnetic coupling in Fe/Cr multilayered structures observed by Unguris *et al.*² or by Demokritov *et al.*⁴ When we consider effects of finite width of the VBS it does not help the $J_{\text{RKKY}}(z)$ coupling look like the experimental data.^{2,4} At best, the width of the VBS can make the coupling oscillate about zero [see Fig. 4(b)], with a realistic finite width

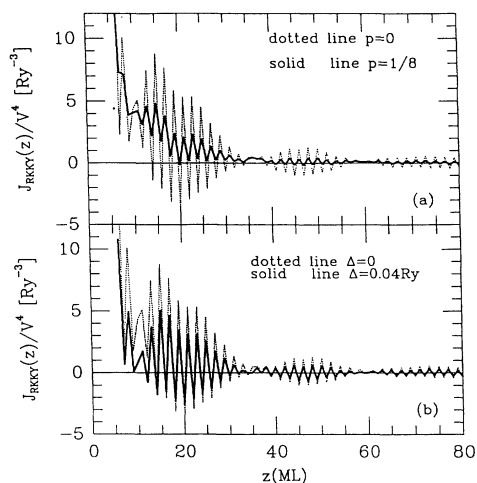


FIG. 4. (a) The RKKY-like interlayer magnetic coupling $\langle J_{\text{RKKY}}(z) \rangle_p$ of Fe/Cr(001) multilayered structures calculated with $E_h = 0.08$ Ry, and $p = 0$ (dotted line) for smooth interfaces and $p = 1/8$ (solid line) for slightly roughened interfaces. The units of coupling J are rydbergs where V is expressed in rydbergs. (b) Comparison of RKKY interlayer magnetic coupling for local state with no broadening and a VBS with $\Delta = 0.04$ Ry for $E_h = 0.08$ Ry, and a smooth interface ($p = 0$). Here positive and negative J represent ferromagnetic and antiferromagnetic coupling, respectively.

$\Delta = 0.04$ Ry; the broadened VBS *reduces* the ferromagnetic bias for small z , but this coupling *cannot* produce the strongly antiferromagnetic interlayer magnetic coupling seen in data at small chromium layer thickness (4–10 ML).^{2,4} Thus *we can conclude that the modified RKKY coupling by itself cannot explain the interlayer magnetic coupling in Fe/Cr multilayered structures.*

However, Wang, Levy, and Fry²⁵ used the two-impurity Anderson model, and obtained the correct behavior for the Fe/Cr interlayer magnetic coupling. The salient contribution that enters the coupling when using this model comes from considering a slowly decaying nonoscillatory superexchange coupling. In the next section we will present two types of excitation mechanisms that appear in the Anderson model and we interpret interlayer magnetic coupling in metallic multilayered structures in terms of these processes.

III. INTERLAYER MAGNETIC COUPLING: RKKY AND SUPEREXCHANGE

We turn now to the possibility that interlayer magnetic coupling contains not only an oscillatory term but also a slowly decaying, nonoscillatory contribution. We will show that both types of coupling can be derived naturally in the two-impurity Anderson model.

In 1972, Goncalves da Silva and Falicov⁴⁷ used the Anderson model to calculate the magnetic coupling in rare earth metals of localized f electrons via the itinerant sp electrons. In fourth-order perturbation theory, their model gave both superexchange and an oscillating RKKY coupling for metallic itinerant bands. Wang, Levy, and Fry²⁵ have proposed that interface states associated with Fe atoms at the interfaces of Fe/Cr multilayered structures produce the magnetic perturbation of the Cr layer that couples the Fe layers. In this calculation, the paramagnetic Cr layer has been modeled by the bulk band structure which has provided a reliable RPA susceptibility.³⁷

In this section we use the two-impurity Anderson model and derive the interlayer magnetic coupling in two ways. First we calculate the interlayer magnetic coupling by applying the Hartree-Fock approximation and by using Green's functions. In a second approach, we follow fourth-order perturbation theory to calculate the interlayer magnetic coupling. Then, we point out the equivalence between Caroli's Green's function method⁴⁵ and fourth-order perturbation theory of the two-impurity Anderson model. Finally, we demonstrate that there are two essentially different types of excitation mechanism needed to interpret interlayer magnetic coupling in the two-impurity Anderson model: low-energy spin excitations, which give rise to the RKKY coupling previously found from the one-site Schrieffer-Wolff transformation, Eq. (12) and Eq. (15), and high-energy virtual charge excitations, which produce a superexchange coupling that *cannot* be derived by the method used in Sec. II.

A. Interlayer magnetic coupling in the Anderson model: Green's function method

The interaction between two magnetic ions in a non-magnetic metal can be represented by the two-impurity

Anderson Hamiltonian

$$H = \sum_{n\mathbf{k}\sigma} \varepsilon_{n\mathbf{k}} C_{n\mathbf{k}\sigma}^\dagger C_{n\mathbf{k}\sigma} + \sum_{i=1,2} \varepsilon_{id\sigma}^0 C_{id\sigma}^\dagger C_{id\sigma} + \sum_{i=1,2,n\mathbf{k},\sigma} (V_{n\mathbf{k}} C_{n\mathbf{k}\sigma}^\dagger C_{id\sigma} + V_{n\mathbf{k}}^* C_{id\sigma}^\dagger C_{n\mathbf{k}\sigma}), \quad (17)$$

where $\varepsilon_{n\mathbf{k}}$ is the energy level for the conduction electrons, $\varepsilon_{id\sigma}^0$ is the energy level for the impurity states, $C_{n\mathbf{k}\sigma}^\dagger$, $C_{n\mathbf{k}\sigma}$ are the creation and annihilation operators for the conduction electrons with spin direction σ , $C_{d\sigma}^\dagger$, $C_{d\sigma}$ are those for the d electrons of the magnetic ions, and $V_{n\mathbf{k}}$ is the strength of mixing interaction between localized and conduction electrons. Generally, there are three approaches to solve this Hamiltonian: (i) a Green's function method, (ii) perturbation theory, and (iii) a canonical transformation like the Schrieffer-Wolff transformation.³⁹

In the Green's function approach the interaction between the magnetic impurities is given by the change in the total (Hartree-Fock) energy of the system due to mixing interaction,⁴⁵ i.e.,

$$E_{\text{int}} = \sum_{\sigma} \int_{-\infty}^{\varepsilon_F} d\varepsilon (\varepsilon - \varepsilon_F) \delta\rho^{\sigma}(\varepsilon), \quad (18)$$

where $\delta\rho^{\sigma}$ is the total density of electron states per unit

energy for spin direction σ . By using the Hartree-Fock approximation and assuming that ion-ion interactions have negligible effects on the occupation of local levels of the magnetic ions Caroli⁴⁵ showed the magnetic interaction between two impurities separated by a distance \mathbf{r} is given by

$$E_{\text{int}}^{\sigma\sigma'} = -\frac{1}{\pi} \text{Im} \int_{-\infty}^{\varepsilon_F} d\varepsilon G_1^{0\sigma}(\varepsilon) F(\varepsilon, \mathbf{r}) G_2^{0\sigma'}(\varepsilon). \quad (19)$$

Here

$$G_i^{0\sigma} = \frac{1}{\varepsilon - \varepsilon_i^{\sigma}} \quad (20)$$

is the Green's function of the local impurity state at site i , ε_i^{σ} is the energy of the local state, and

$$F(\varepsilon, \mathbf{r}) = \sum_{n_1\mathbf{k}} \frac{V_{1,n_1\mathbf{k}} V_{n_1\mathbf{k},2}}{\varepsilon - \varepsilon_{n_1\mathbf{k}}} \sum_{n_2\mathbf{k}'} \frac{V_{2,n_2\mathbf{k}'} V_{n_2\mathbf{k}',1}}{\varepsilon - \varepsilon_{n_2\mathbf{k}'}} \quad (21)$$

represents the coupling between two impurity states through the electron gas, where $V_{n_1\mathbf{k},i} = e^{-i\mathbf{k}\cdot\mathbf{r}_i} V_{n_1\mathbf{k},O}$, and O represents the origin. Then the coupling energy (the energy difference between ferro- and antiferromagnetic configurations) is

$$J(\mathbf{r}) = -\frac{1}{\pi} \text{Im} \sum_{\sigma\sigma'} \sum_{n_1\mathbf{k}, n_2\mathbf{k}'} \sigma\sigma' \int_{-\infty}^{\varepsilon_F} d\varepsilon \frac{|V_{n_1\mathbf{k}}|^2 |V_{n_2\mathbf{k}'}|^2 e^{i(\mathbf{k}'-\mathbf{k})\cdot\mathbf{r}}}{(\varepsilon - \varepsilon_1^{\sigma})(\varepsilon - \varepsilon_{n_1\mathbf{k}})(\varepsilon - \varepsilon_{n_2\mathbf{k}'})(\varepsilon - \varepsilon_2^{\sigma'})} \quad (22)$$

and is equal to $I_{\text{eff}} S^2$. The energy difference between ε_i^{\uparrow} and $\varepsilon_i^{\downarrow}$ is the order of the intra-atomic Coulomb interaction U ; as discussed in the following paragraph we take the large U limit. The lower energies for local states of two impurities are set to be equal to ε_l . The integration that picks up poles related to the conduction band at $\varepsilon = \varepsilon_{n_1\mathbf{k}}$ or $\varepsilon = \varepsilon_{n_2\mathbf{k}'}$ gives the RKKY-like coupling whose form in reciprocal space is

$$J_{\text{RKKY}}(\mathbf{q}) = \sum_{n_1, n_2, \mathbf{k}} \left[\frac{|V_{n_1\mathbf{k}}|^2 |V_{n_2\mathbf{k}'}|^2}{(\varepsilon_{n_2\mathbf{k}'} - \varepsilon_l)^2} \frac{\theta(\varepsilon_f - \varepsilon_{n_1\mathbf{k}}) \theta(\varepsilon_{n_2\mathbf{k}'} - \varepsilon_f)}{\varepsilon_{n_2\mathbf{k}'} - \varepsilon_{n_1\mathbf{k}}} + \text{c.c.} \right], \quad (23)$$

where $\mathbf{k}' = \mathbf{k} + \mathbf{q} + \mathbf{G}$ and \mathbf{G} is a vector of the reciprocal lattice. One sees that this reproduces the RKKY interaction Eq. (12) when one relates $V_k^2/(\varepsilon_k - \varepsilon_l)$ to I_k . The additional contribution from the poles related to *local states* at $\varepsilon = \varepsilon_l$ gives an antiferromagnetic coupling whose Fourier transform is

$$J_S(\mathbf{q}) = - \sum_{n_1, n_2, \mathbf{k}} \left[\frac{|V_{n_1\mathbf{k}}|^2 |V_{n_2\mathbf{k}'}|^2}{(\varepsilon_{n_2\mathbf{k}'} - \varepsilon_l)^2} \frac{\theta(\varepsilon_{n_1\mathbf{k}} - \varepsilon_f) \theta(\varepsilon_{n_2\mathbf{k}'} - \varepsilon_f)}{\varepsilon_{n_1\mathbf{k}} - \varepsilon_l} + \text{c.c.} \right]. \quad (24)$$

This is a new term called superexchange coupling,⁴⁷ and is not within the paradigm of the RKKY interaction discussed in Sec. II.

The local states ε_l of a magnetic impurity lying below and above the Fermi level ε_F correspond to occupied and unoccupied states, respectively. Suppose one electron, say, with spin down, occupies the local state ε_d which lies below the Fermi surface. The presence of a spin-down electron in an orbitally nondegenerate local state excludes another spin-down electron, and there is also a repulsive field for spin up due to the intra-atomic Coulomb interaction U . Therefore, the energy level for the spin-up state will lie at $\varepsilon_d + U$. That state is above the Fermi level if U is large enough. We set $\varepsilon_+ = \varepsilon_d + U$

to represent the local state below the Fermi level ε_F , and $\varepsilon_- = \varepsilon_d + U$ for a local state above ε_F . Σ_d is a self-energy correction and at the level of our approximation has no σ dependence. Anderson³⁸ pointed out that it is the ratio of the intra-atomic Coulomb interaction U to the mixing interaction $V_{n\mathbf{k}}$ that determines whether a local magnetic moment in a metallic host can be formed or not. For rare earth metallic compounds, the on-site Coulomb interaction U is very strong, so that they always exhibit magnetic moments. Similarly, we will use a large U limit in case of magnetic multilayered structures, because the magnetic moments in the magnetic layers are quite large, e.g., iron. From electronic structure calculations of magnetic impurities in nonmagnetic metals,

it is reasonable in a first approximation to focus on local states ε_+ below and closer to ε_F , and to neglect the process of absorbing an electron from the Fermi sea in an unoccupied local level ε_- which is above but farther away from ε_F .⁴⁸ The contribution to the coupling from unoccupied local states above ε_F is small, especially in the large U limit; therefore we set $\varepsilon_l = \varepsilon_+$ in the numerical calculations in following sections. When these unoccupied local states above ε_F are included in our calculations they do *not* change any of our results.

The merit of the Green's function method is that it can

$$\langle J_t(z) \rangle_p = \frac{a}{2\pi} \int_0^\infty f_1(q_z) f_2(q_z) |j_t(q_z)| \cos[q_z z + \varphi(q_z)] dq_z, \quad (26)$$

where $|j_t(q_z)| = \sqrt{\{\text{Re}[j_t(q_z)]\}^2 + \{\text{Im}[j_t(q_z)]\}^2}$, and $\varphi(q_z) = \tan^{-1}\{\text{Im}[j_t(q_z)] / \text{Re}[j_t(q_z)]\}$.

B. Canonical transformation and fourth-order perturbation theory for two-impurity Anderson model

A two-site canonical transformation which obtains the same result is related to the Schrieffer-Wolff canonical transformation³⁹ which converts the Anderson Hamiltonian³⁸ into an effective spin Hamiltonian in the limit where one conserves the number of local electrons. In this limit, known as the Kondo limit, the local moment is well defined. The basic idea of the Schrieffer-Wolff transformation is to remove the mixing interaction to first order. Then, the first nonzero contribution from the interaction between conduction and localized electrons is proportional to square of mixing strength V_{nk}^2 . To couple two impurities at different sites, one has to calculate the effects of the mixing interaction to fourth

pick up all eigenstates of the system, which are related to poles in the integration. The local states and conduction electron states together form a complete set of eigenstates of the two-impurity Anderson Hamiltonian. One sees that the total coupling in reciprocal space can be written down as

$$j_t(\mathbf{q}) = j_{\text{RKKY}}(\mathbf{q}) + j_S(\mathbf{q}). \quad (25)$$

Its form in real space is obtained in a way similar to that used for Eq. (16),

order.^{46,49} The idea is to perform successive canonical transformations aimed at eliminating odd powers of the mixing parameter V_{nk} . The transformed Hamiltonian has the form

$$\tilde{H} = \dots e^{S^3} e^{S^1} H e^{S^1} e^{S^3} \dots, \quad (27)$$

where $H = H_0 + V$, and the superscript $(2m+1)$ on S indicates the order in V_{nk} of each successive term. To eliminate V_{nk} to first order in \tilde{H} , S^1 must satisfy the relation $[H_0, S^1] = V$, as in the Schrieffer-Wolff case. The next higher-order terms generated by S^3 describe third-order hybridization effects. To eliminate them, one chooses S^3 such that $[H_0, S^3] = \frac{1}{2}[S^1, [S^1, V]]$. Then the transformed Hamiltonian, containing only second- and fourth-order terms in V_{nk} , is

$$H_{\text{eff}} = H^{(0)} + H^{(2)} + H^{(4)} + \dots \quad (28)$$

The matrix elements of $H^{(2)}$ and $H^{(4)}$ between eigenstates of $H^{(0)}$ are

$$\begin{aligned} \langle a | H^{(2)} | b \rangle &= \frac{1}{2} \sum_c V_{ac} V_{cb} (D_{ac} - D_{cb}), \\ \langle a | H^{(4)} | b \rangle &= \frac{1}{8} \sum_{cde} V_{ac} V_{cd} V_{de} V_{eb} (D_{ac} D_{cd} D_{de} - D_{cd} D_{de} D_{eb} + 3D_{ac} D_{de} D_{eb} - 3D_{ac} D_{cd} D_{eb}), \end{aligned} \quad (29)$$

where $D_{ij} = (E_i - E_j)^{-1}$ and $V_{ab} = \langle a | V | b \rangle$. Then, the coupling is written down as

$$E^{(4)} = \sum_d H_{id}^{(2)} H_{df}^{(2)} D_{id} + H_{if}^{(4)}, \quad (30)$$

where $|i\rangle$ and $|f\rangle$ are degenerate ground states of $H^{(0)}$ for the two sites. By inserting Eq. (29) into Eq. (30) one obtains

$$E^{(4)} = \sum_{cde} V_{ic} V_{cd} V_{de} V_{ef} D_{ic} D_{id} D_{ie}. \quad (31)$$

This resembles the conventional fourth-order perturbation theory result. However, the denominators contain the mixing parameter V_{nk} ; therefore Eq. (31) is not simply fourth order in the mixing interaction.⁴⁶ It is worth

pointing out that Eq. (31) contains contributions from all possible intermediate states. It is not difficult to sort out the coupling strengths $j_{\text{RKKY}}(q)$ and $j_S(q)$, which are discussed in Refs. 46 and 49.

In conclusion, we point out that results found for the s - d model by using Caroli's Green's function method can be reproduced with this two-site canonical transformation.

C. Spin and virtual charge excitations

The physical picture of the RKKY (j_{RKKY}) and superexchange (j_S) couplings is related to two basic excitations in the two-impurity Anderson Hamiltonian. The coupling $j_{\text{RKKY}}(q)$ comes only from intermediate states which correspond to *spin excitations*, as shown in Fig. 5,

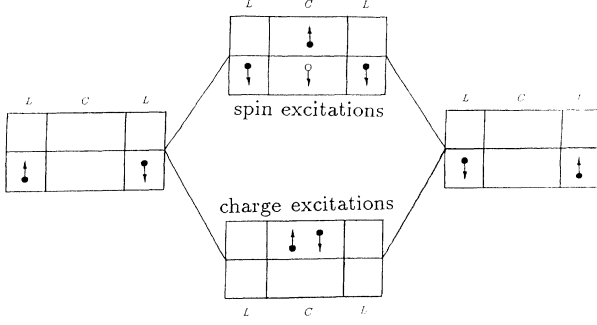


FIG. 5. Schematic diagram for spin and charge excitations in two-impurity Anderson model. L and C represent local impurity and conduction electron states, respectively.

of the Fermi sea, i.e., states which correspond to electron-hole pair production in the Fermi sea with attendant spin flip.^{46,47} This coupling is largely influenced by the Fermi surface through the denominator $(\varepsilon_{n_2 k'} - \varepsilon_{n_1 k})$ in Eq. (23), which is singular when both states $(n_1 k$ and $n_2 k')$ are infinitesimally close to the Fermi surface. Thus, the topology of the Fermi surface generates peaks and structure in $j_{\text{RKKY}}(q)$, which come from stationary wave vectors which span the Fermi surface. These stationary wave vectors translate into oscillations of the interlayer magnetic coupling in real space, $J_{\text{RKKY}}(z)$.

The coupling $j_S(q)$ arises from *virtual-charge excitations*, as shown in Fig. 5, which have electrons from local states above the Fermi sea (one from each layer); it provides a second contribution to the coupling, that is, in addition to the RKKY coupling.^{25,27} $j_S(q)$ does

not contain much Fermi-surface (oscillatory) information. For narrow virtual bound states, there are no peaks and structure in $j_S(q)$ because both states, $n_1 k$ and $n_2 k'$, are above the Fermi surface; that is, they have no chance of touching the Fermi surface. When one considers effects of finite widths of the VBS, there will be a small oscillation along with the strongly antiferromagnetic coupling $J_S(z)$, because the tail of the virtual bound state touches (crosses) the Fermi surface. In the following two sections, we will further investigate these two types of couplings.

IV. INTERLAYER MAGNETIC COUPLING IN THE FREE ELECTRON GAS APPROXIMATION

Before attempting to calculate the coupling for a particular band structure, it is of pedagogical value to study it within the free electron gas approximation. Since this approximation *may* be suitable for noble-metal spacer layers, we consider a fcc host material with one conduction electron per atom. Then the Fermi vector is $k_F = (12\pi^2)^{1/3}/a$, where a is the lattice constant, e.g., $k_F = 0.78(2\pi/a)$.

A. RKKY and superexchange couplings in the free electron gas approximation

First we discuss the narrow virtual bound state limit, i.e., $\Delta = 0$, and consider one local level below ε_F for simplicity. Then $j_{\text{RKKY}}(q)$ in Eq. (23) and $j_S(q)$ in Eq. (24) can be evaluated analytically without any approximation,

$$j_{\text{RKKY}}(q) = \frac{vV^4}{16\pi^2 q} \left[\frac{1}{k_F^2 - k_0^2} \ln \left| \frac{(k_F + q)^2 - k_0^2}{k_F^2 - k_0^2} \right| - \frac{1}{k_F^2 - k_0^2} \ln \left| \frac{q + 2k_F}{q - 2k_F} \right| \right. \\ \left. + \frac{1}{k_0(q + 2k_0)} \ln \left| \frac{k_F + q + k_0}{k_F + k_0} \right| + \frac{1}{k_0(q + 2k_0)} \ln \left| \frac{q - 2k_F}{q + 2k_F} \right| \right. \\ \left. - \frac{1}{k_0(q - 2k_0)} \ln \left| \frac{k_F + q - k_0}{k_F - k_0} \right| - \frac{1}{k_0(q - 2k_0)} \ln \left| \frac{q - 2k_F}{q + 2k_F} \right| \right] \quad (32)$$

and

$$j_S(q) = -\frac{vV^4}{16\pi^2 q} \left[\frac{1}{k_F^2 - k_0^2} \ln \left| \frac{(k_F + q)^2 - k_0^2}{k_F^2 - k_0^2} \right| + \frac{1}{k_0(q + 2k_0)} \ln \left| \frac{k_F + q + k_0}{k_F - k_0} \right| - \frac{1}{k_0(q - 2k_0)} \ln \left| \frac{k_F + q - k_0}{k_F + k_0} \right| \right], \quad (33)$$

where v is volume of a primitive cell of the lattice, $k_0 = \sqrt{2m(\varepsilon_F - E_h)}$ is a momentum of local impurity states, and $k_F = \sqrt{2m\varepsilon_F}$ is the Fermi momentum of the electron gas. The total coupling j_t is easily obtained as

$$j_t(q) = -\frac{vV^4}{16\pi^2(q^2 - 4k_0^2)} \left[\frac{2}{k_0} \ln \left| \frac{k_F + k_0}{k_F - k_0} \right| + \frac{q^2 - 4k_F^2}{q(k_F^2 - k_0^2)} \ln \left| \frac{q + 2k_F}{q - 2k_F} \right| \right], \quad (34)$$

and agrees with the coupling derived by Proetto and López.⁴⁹

In Fig. 6, we plot $j_{\text{RKKY}}(q)$ and $j_S(q)$ for $E_h = 0.1\varepsilon_F$. In the previous section we pointed out that $j_{\text{RKKY}}(q)$ contains structures which come from the extremal wave

vectors across the Fermi surface. One notices that $j_{\text{RKKY}}(q)$ has a dip at $q = 2k_F = 1.56(2\pi/a)$, while $j_S(q)$ is a smooth curve. Figure 7 shows their Fourier transforms, namely, $J_{\text{RKKY}}(z)$ and $J_S(z)$. One can see that the $J_{\text{RKKY}}(z)$ oscillates with a short period $\lambda = 1.3$

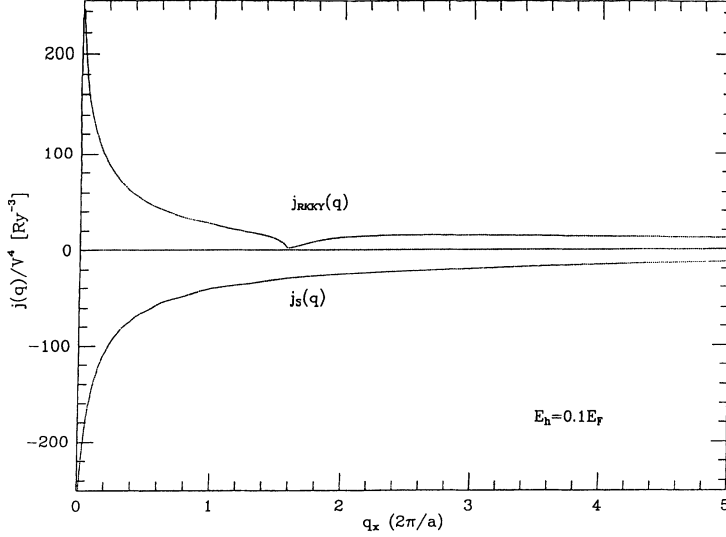


FIG. 6. RKKY-like coupling $j_{\text{RKKY}}(q)$ and superexchange coupling $j_S(q)$ in the free electron gas approximation calculated with $E_h = 0.1\epsilon_F$, and $\Delta = 0$.

ML, which corresponds to the dip $q = 2k_F$ ($q\lambda = 2\pi$) in reciprocal space. It is interesting to note that $J_{\text{RKKY}}(z)$ is strongly ferromagnetically biased when we choose for the energy dependence of $I_{n_1 k, n_2 k'}$ [Eq. (15)]. When one treats $I_{n_1 k, n_2 k'}$ as a constant $J_{\text{RKKY}}(z)$ reduces to a conventional RKKY oscillatory coupling without ferromagnetic bias. On the other hand, $J_S(z)$ is a monotonic antiferromagnetic coupling which does not contain oscillatory information, as one expects, because it comes from states away from the Fermi surface. When we put $J_{\text{RKKY}}(z)$ and $J_S(z)$ together we find the conventional RKKY pattern which means that the antiferromagnetic $J_S(z)$ cancels the ferromagnetic bias in $J_{\text{RKKY}}(z)$, at least for a free electron gas.

B. Aliasing effect

When we sample $J_t(z)$ at lattice sites for fcc host material we find that the short-period oscillation $\lambda = 1.3$ ML translates as a long-range oscillation with period $\lambda = 4.6$

ML which corresponds to $q = G - 2k_F$ in reciprocal space [$G = 4\pi/a$ for fcc in the (001) direction]; i.e., we have an aliasing effect as shown in Fig. 8. This effect has been discussed by several authors in the context of magnetic multilayers.^{26,50,51} Actually, this aliasing effect can be understood from the theory of Fourier analysis.²³

From the above considerations, it is obvious that any calculation including lattice periodicity contains the aliasing effect automatically, which is important in obtaining long-period oscillations of the interlayer magnetic coupling. In particular, tight-binding calculations which include the lattice structure, *ab initio* calculations, and calculations based on real band structures naturally contain this effect and thereby long-period oscillations.

C. Effect of virtual bound states

We have calculated $J_{\text{RKKY}}(z)$ for $E_h = 0.1\epsilon_F$, with $\text{Im}[\epsilon_+] = \Delta = 0, 0.5E_h$ and $2.0E_h$, as shown in Fig. 9. The results are consistent with those found in Sec. II.

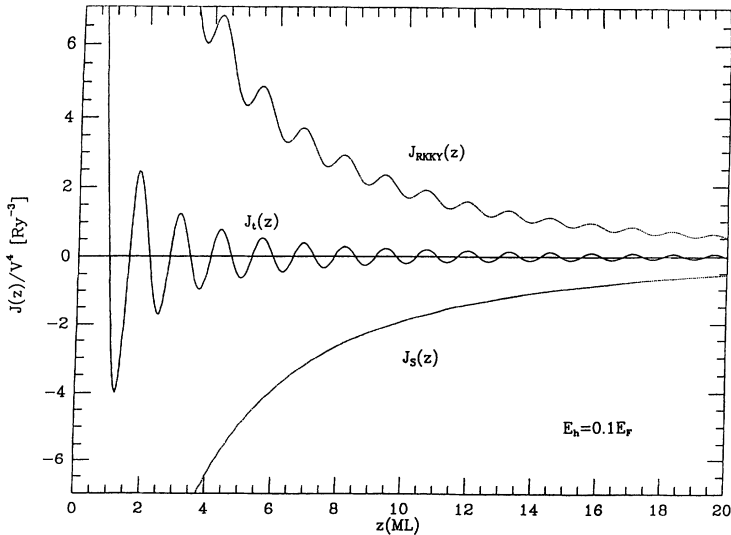


FIG. 7. RKKY-like $J_{\text{RKKY}}(z)$, superexchange $J_S(z)$, and total coupling $J_t(z)$ in the free electron gas approximation as a function of thickness of spacer z , calculated with $E_h = 0.1\epsilon_F$ and $\Delta = 0$.

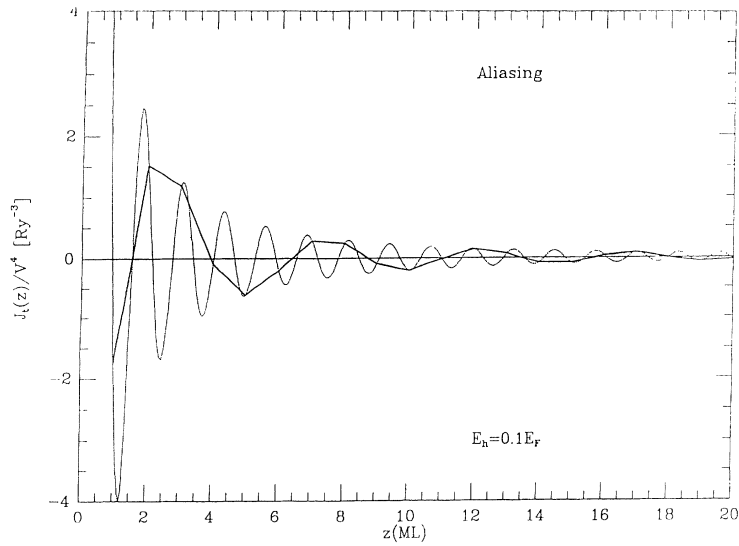


FIG. 8. Comparison of total coupling $J_t(z)$ in continuous space and for sampling at lattice sites.

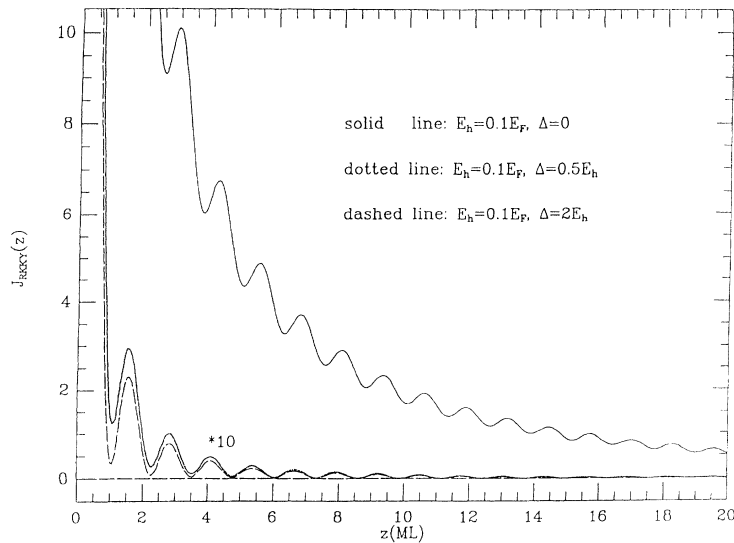


FIG. 9. The effects of virtual bound states on RKKY-like coupling $J_{\text{RKKY}}(z)$.

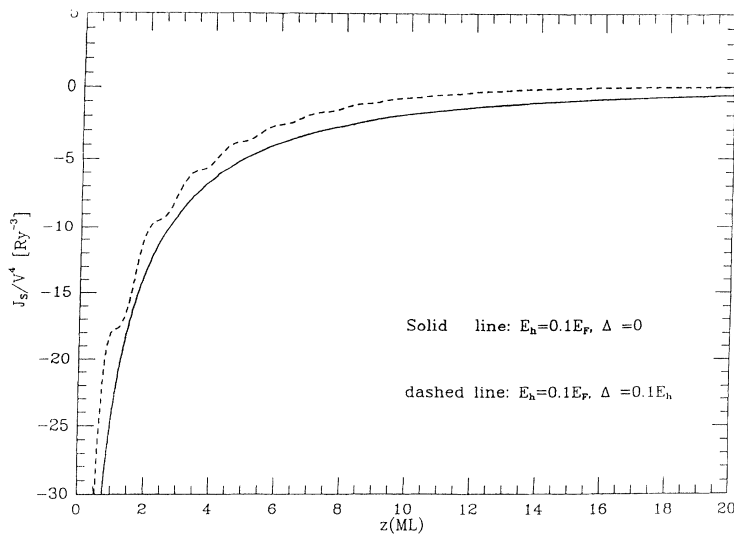


FIG. 10. The effects of virtual bound states on superexchange coupling $J_S(z)$.

The effect of the broadening of a VBS on $J_S(z)$ is to add small oscillations to the antiferromagnetic coupling $J_S(z)$, as shown in Fig. 10, because the tail of the VBS crosses the Fermi surface. We have varied E_h and found that it does not alter the conclusions discussed in this section.

D. Bias of the interlayer magnetic coupling

The RKKY coupling, an indirect coupling between two magnetic ions or magnetic layers embedded in a nonmagnetic metal, is found in a second-order perturbation treatment with respect to $I_{n_1 k, n_2 k'}$ (fourth order in V_{nk}), of the free electron gas, and it exhibits oscillatory features. When they restricted themselves to evanescent states Dreyfus *et al.*⁵² demonstrated that it is possible for an induced spin density with a bias to exist in a nonmagnetic layer. They suggested that the difference between their conclusion and RKKY coupling resulted from the nonperturbative nature of the problem which they treated. Bardasis *et al.*⁵³ and Yosida and Okiji⁵⁴ reexamined the calculation of Dreyfus *et al.*⁵² by evaluating an additional contribution from *nonevanescence* states to the spin density. They found that the nonevanescence states contribute a nonoscillatory spin polarization which exactly cancels that coming from the evanescent states, thereby leaving the expected RKKY oscillatory spatial dependence without any bias.

Recently, Erickson, Hathaway, and Cullen¹⁵ studied the cancellation of the nonoscillatory terms to the coupling by calculating the torque acting on the spin-flip current in a magnetic/nonmagnetic/magnetic sandwich. They also employed a free electron gas for the magnetic and nonmagnetic layers, and in magnetic layers they considered the conduction band split by an exchange interaction into spin-up and spin-down subbands as did Dreyfus *et al.*,⁵² Bardasis *et al.*,⁵³ and Yosida-Okiji.⁵⁴ We use the *s-d* mixing interaction at the interfaces to study the interlayer magnetic coupling. This is a different mechanism to induce the spin polarization and we model the magnetic ion or layer as a local level, and the nonmagnetic metal as an electron gas. In Sec. IV A we saw that the ferromagnetic bias of $J_{\text{RKKY}}(z)$ is exactly canceled by antiferromagnetic $J_S(z)$ and gives a conventional RKKY-like coupling $J_t(z)$ as shown in Fig. 7. Therefore, it seems that the cancellation property may be universal, i.e., irrespective of whether it is treated by perturbative or nonperturbative methods, and results from considering the complete set of the eigenstates of a system.^{53,54}

For the spin-dependent scattering at the interface when one considers $I_{n_1 k, n_2 k'}$ in Eq. (2) to be a constant, the complete set of eigenstates of the system consists only of the conduction bands of the nonmagnetic spacer. The coupling (RKKY) from it is a conventional oscillatory coupling without bias. When $I_{n_1 k, n_2 k'}$ comes from the *s-d* mixing interaction it has the form of Eq. (15); therefore it is not a constant; also the complete set of eigenstates is a combination of local states from the magnetic layers and the conduction bands of the nonmagnetic spacer. Then it is not too surprising that the RKKY-like coupling $J_{\text{RKKY}}(z)$ in Sec. II is biased. From the Green's function

method in Sec. III one realizes that it results from a subset (conduction bands) of the complete set of the eigenstates. The other part of the coupling $J_S(z)$, coming from another subset (local levels), is antiferromagnetic and, as we showed in Sec. IV A cancels the ferromagnetic bias, *at least for a free electron gas*. One could posit that this cancellation property comes from the existence of a parabolic band, the use of constant matrix elements, or both, but what happens for realistic nonparabolic band structures? Wang, Levy, and Fry²⁵ studied the interlayer magnetic coupling in Fe/Cr/Fe multilayered structures based on the paramagnetic Cr band structure. They found $J_S(z)$ does *not* completely cancel the ferromagnetic bias $J_{\text{RKKY}}(z)$, but leaves some antiferromagnetic bias. The violation of the complete cancellation may come from the nonparabolicity of the band structure, from the behavior of the matrix elements, or yet for some other reasons. This point will be clarified in the next section.

V. INTERLAYER MAGNETIC COUPLING IN IRON/CHROMIUM MULTILAYERED STRUCTURES

Several experiments have demonstrated that spin polarization is induced in Cr by a magnetic Fe layer^{41,42} and that the magnetic layers are coupled in Fe/Cr/Fe multilayered structures.^{2,42} On the other hand, additional experimental data have shown that spin polarization and interlayer magnetic coupling patterns are not identical, a finding that can be construed to imply that the RKKY-like coupling alone is not enough to account for the observed interlayer magnetic coupling. In this section we discuss whether the superexchange coupling is sufficient, in addition to the RKKY coupling, to explain experimental data on the coupling of Fe/Cr multilayered structures.

A. Matrix elements

At the large distance, the coupling $j(q)$ should be proportional to $\chi(q)$ because the details of the local-moment-conduction-electron interaction do not matter; i.e., for large R_{AB} (distance between two impurities A and B), the only contribution to the indirect coupling comes from low-energy spin excitations of the Fermi sea. Due to Fermi factors these occur for $q \rightarrow 0$ at $k = k_F$. Thus, for the large R_{AB} behavior of the interlayer magnetic coupling one can write $|V_{n_1 k}|^2 |V_{n_2 k'}^*|^2 = V^4 |M_{n_1 k, n_2 k'}(\mathbf{q})|^2$ for small q so that $j_{\text{RKKY}}(q)$ [see Eq. (23)] is proportional to $\chi(q)$. However, for the short-range behavior (large q), there is no reason to keep this identification; for large q , the V_{nk} 's should be chosen to reflect the fact that they represent the *s-d* mixing interaction whose range is quite short (local) within one unit cell (the one the impurity occupies). For large q , the choice $|V_{n_1 k}|^2 |V_{n_2 k'}^*|^2 = \text{const}$ makes sense, because upon taking its Fourier transform, it represents the coupling of a pointlike interaction.

In summary, for small q , one can make the identification of the V_{nk} 's with the form factor matrix elements,

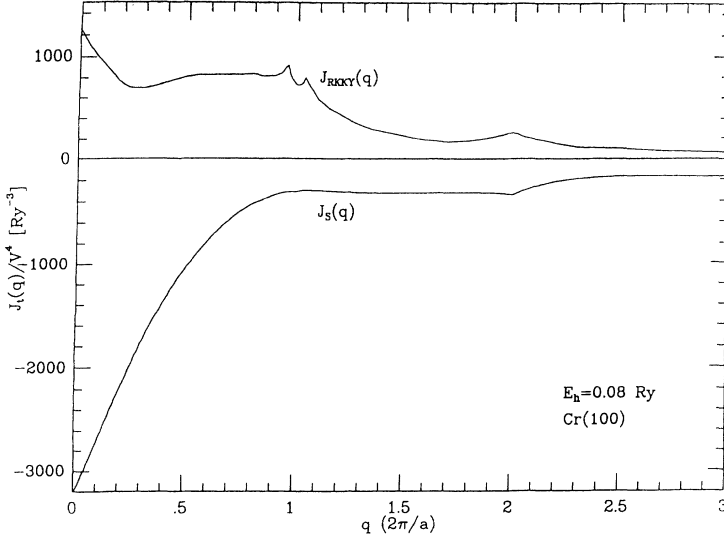


FIG. 11. RKKY-like $j_{\text{RKKY}}(q)$ and superexchange coupling $J_S(q)$ for Cr(001) in reciprocal space calculated with $E_h = 0.08$ Ry and $\Delta = 0$. V is expressed in rydbergs.

whereas for large q one should take them to be constants to reproduce a pointlike excitation; of course, in between one must interpolate. One approximation is to choose the s and p form factors as constant throughout the whole q space—far past the region where the true form factor $M_{n_1 k, n_2 k'}(q)$ exists for s and p electrons.

B. Coupling in Fe/Cr multilayered structures

With these approximations, and based on the band structure of bulk paramagnetic Cr, we have calculated the couplings $j_{\text{RKKY}}(q_z)$ and $j_S(q_z)$ (q_z is along the ΓH direction in reciprocal space for the bcc lattice), [see Eqs. (23) and (24)] with $E_h = 0.08$ Ry (the coupling calculated from this value resembles the experimental data^{25,27}) as shown in Fig. 11. The twin peaks in $j_{\text{RKKY}}(q)$ reproduce the incommensurate SDW instability occurring at $q_{\text{SDW}} \simeq 0.958\Gamma H$ and $1.042\Gamma H$ in Cr.³⁷ The dip in $j_{\text{RKKY}}(q)$ for $q_1 \simeq 0.2(2\pi/a)$ corresponds to the wave vector across the Fermi surface shown in Fig. 12.

When we take into account the roughness of interfaces,

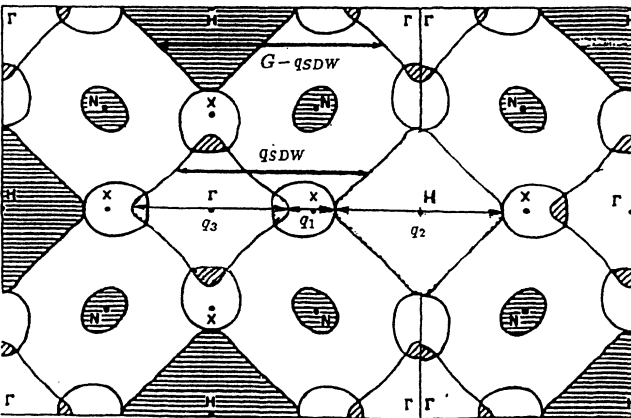


FIG. 12. The Fermi cross section for Cr(001) (Ref. 43). Five extremal wave vectors are indicated.

the interlayer magnetic coupling Eq. (26) has the following form:

$$\langle J_t(n) \rangle_p = (1-2p) J_t(n) + p [J_t(n+1) + J_t(n-1)] \quad (35)$$

where n is a label for the lattice site. In Fig. 13, we show results on $\langle J_t \rangle_p$ (the total coupling) for smooth ($p = 0$), irregular (not very rough, $p = 1/8$), and rough ($p = 1/4$) interfaces. One sees that there is a 2 ML rapid oscillation for smooth interfaces which corresponds to the peak at q_{SDW} in $j_{\text{RKKY}}(q)$. The coupling for rough interfaces ($p = 0.25$) is

$$\langle J_t(n) \rangle_{p=0.25} = \frac{1}{2} [J_t(n+1) + J_t(n-1) + 2J_t(n)] \quad (36)$$

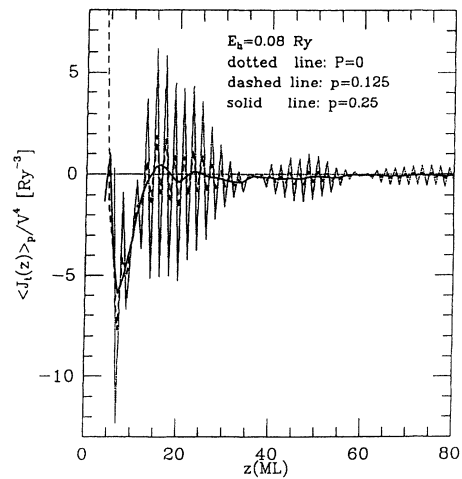


FIG. 13. The total interlayer magnetic coupling $\langle J_t(z) \rangle_p$ of Fe/Cr(001) multilayered structures calculated with $E_h = 0.08$ Ry, $\Delta = 0$, and $p = 0$ (dotted line) for smooth interfaces and $p = 1/8$ (dashed line) for slight rough interfaces, and $p = 0.25$ for rough interfaces. Here positive and negative J represent ferromagnetic and antiferromagnetic coupling, respectively.

This expression attenuates short-period oscillations while it retains those with longer periods. The 10 ML long-range oscillation for $\langle J_t(n) \rangle_{p=0.25}$ (see Fig. 13) corresponds to the long-wavelength oscillation observed in Fe/Cr multilayered structures²⁻⁴ and is related to the dip at $q_1 \simeq 0.2(2\pi/a)$ in $j_{\text{RKKY}}(q)$ (see Fig. 11).

C. Remark on interfacial roughness

Adding roughness at the interface can have dramatic effects on the calculated interlayer magnetic coupling. Wang, Levy, and Fry²⁵ first introduced the concept of interface roughness in conjunction with interlayer magnetic coupling when they studied the coupling in Fe/Cr(001) multilayered structures. They predicted that the roughness of the interface attenuated the rapid oscillations induced by the SDW ordering wave vector. The recent observations^{2,4} of both short- and long-period oscillations in Fe/Cr/Fe systems prepared to reduce interfacial roughness show that roughness may indeed mask short-period oscillations. It implies that one effect of interface roughness on the interlayer magnetic coupling is the attenuation of rapidly oscillating waves, thus making the longer-period oscillations more apparent. Another application for which roughness may play an essential role is the theory of biquadratic coupling proposed by Slonczewski⁵⁵ to explain the preferred 90° alignment of the magnetizations in adjacent ferromagnetic layers observed in several systems.^{2,56,57}

D. Comment on enhancement

The mixing strength V_{nk} in the Anderson model is a parameter. In order to calculate the correct strength of the interlayer magnetic coupling from Eqs. (23)–(25) that can be compared with experimental data, one should include the enhancement factor of the susceptibility due to the interactions between conduction electrons. Within the generalized random phase approximation, Wolff⁵⁸ investigated the effects of electron-electron interactions on the spin susceptibility of an electron gas in the paramagnetic state, and concluded that in an electron gas of density comparable to that found in nonmagnetic metals, the enhancement of the RKKY susceptibility by exchange scattering is not particularly large. Typically, one may expect enhancement factors in the range 1.25–2.0. However a many-body (exchange) enhancement is really needed to discuss *magnetic* metals such as Cr. Its effect on the susceptibility $\chi(q)$ has been worked out by Schwartzman *et al.*,⁵⁹ and can eventually be incorporated into calculation for $j_{\text{RKKY}}(q)$; however, the many-body effects on $j_S(q)$ has not yet been worked out. Callaway and Chatterjee⁶⁰ argued that spin and charge response functions have the same form of enhancement factors as in the case of a paramagnetic material. Here $j_{\text{RKKY}}(q)$ is referred to as *spin excitations* and $j_S(q)$ is referred to as *charge excitations* in the two-impurity Anderson model. Thus, one can expect that the enhancement for the superexchange coupling is the same as for the RKKY coupling. In fact, a countervailing effect is that interfacial roughness attenuates the strength of the interlayer mag-

netic coupling. Due to lack of more detailed information on roughness, it is not realistic to make a comparison of the magnitude of the coupling we predict with experimental results.

E. Oscillatory modes in Fe/Cr/Fe(001) multilayered structures

For Cr the structure of $j_{\text{RKKY}}(q_z)$ contains a dip and twin peaks, as shown in Fig. 11. The dip comes from the extremal wave vector $q_1 = 0.2(2\pi/a)$ of ΓH with opposite z components of the velocity on the Fermi surface, and the twin peaks come from the strong nesting feature of Cr which gives a SDW wave vector $q_{\text{SDW}} = 0.958 \cdot 2\pi/a$ or $G - q_{\text{SDW}} = 1.042(2\pi/a)$ ($G = 4\pi/a$) with the same sign of the z components of velocities on the Fermi surface. These short- and long-range oscillations have been found in experiments.²⁻⁴ However, there are other extremal wave vectors across the Fermi surface with opposite velocities one could identify in Fig. 12 and which are not apparent in $j_{\text{RKKY}}(q_z)$, e.g., $q_2 = 0.8(2\pi/a)$ (inside H) which corresponds to a 2.5 ML oscillation, and $q_3 = 0.75(2\pi/a)$ (inside Γ) which corresponds to a 2.7 ML oscillation. The nesting features for q_2 and q_3 appear to be the same as q_1 . The obvious difference between them is that q_1 is *interband* contribution, but the extremal wave vectors q_2 and q_3 are related to an *intra-band* contribution. The intra-band contributions may be much smaller than interband ones for relatively large scanning wave vector q_z because of the atomic form factor matrix elements, as discussed by Gupta and Sinha.⁶¹ Therefore, the putative structure due to q_2 and q_3 in j_{RKKY} might be lost because of their small contributions.

F. Bias of the interlayer magnetic coupling

In the previous section, we mentioned that from considerations of the completeness of eigenstates of a system one concludes that the oscillatory interlayer magnetic coupling does not have a bias. However, when we take a small $E_h \leq 0.08$ Ry, the interlayer magnetic coupling Eq. (36) for Fe/Cr is strongly antiferromagnetic biased,²⁵ as shown in Fig. 14. The closer the local state is to the Fermi surface, the larger is the antiferromagnetic bias. However, when we change the E_h in the *free* electron approximation, it does not give any bias of the total coupling, as shown in Fig. 15. Thus, an interesting question arises: What are the reasons for the antiferromagnetic bias in realistic Fe/Cr/Fe(001) calculations?

Watson and Freeman⁶² studied exchange coupling and conduction electron polarization in metals with and without an exchange enhancement, and showed that the enhancement produces a large bias. Giovannini *et al.*⁶³ argued that the exchange interaction between the itinerant d electrons produces long-range polarization in metals and large susceptibilities. They considered the exchange correction to the RKKY potential, and conveyed the impression that the enhancement factor induces a bias. We have considered the enhancement factor in the Anderson model and find it does *not* produce a bias.

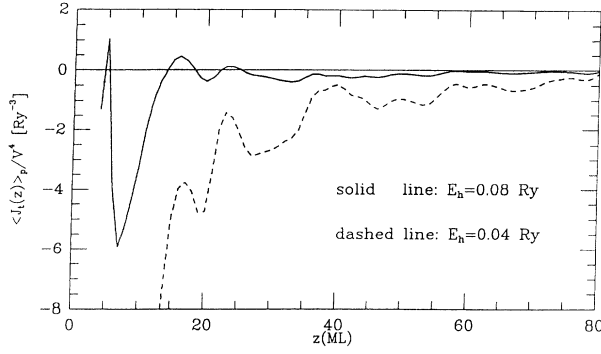


FIG. 14. The total interlayer magnetic coupling $\langle J_t(z) \rangle_p$ of Fe/Cr(001) multilayered structures calculated with $p = 0.25$. The solid line is for $E_h = 0.08 \text{ Ry}$ while the dashed line with the large antiferromagnetic bias is for $E_h = 0.04 \text{ Ry}$ (which is relatively close to the Fermi surface).

One apparent difference between the free electron gas and realistic bands is that the former is parabolic, whereas a realistic band structure is not. To clarify this idea, we consider a nonparabolic band $E = k^2 + ak^3 + bk^4$ instead of a parabolic one $E = k^2$ (in the free electron gas approximation). When we vary the coefficients a and b , we still find no bias.

The choice of matrix elements $M_{n_1 k, n_2 k'}(\mathbf{q})$ has already been discussed in the calculation of the interlayer magnetic coupling.²⁷ Generally, one takes a complicated matrix element for a realistic coupling calculation. Could this be the origin of the bias in the coupling? When we use constant matrix elements in our Fe/Cr/Fe coupling calculation we still find an antiferromagnetic bias for relatively small E_h .

The dominance of antiferromagnetic coupling is a consequence of the size of the average value of the RKKY coupling $[J_{\text{RKKY}}(z)]$ relative to that of the superexchange coupling $[J_S(z)]$. These, in turn, are related to the relative sizes of $j_{\text{RKKY}}(q)$ and $j_S(q)$ at $q = 0$ [$\int J(z) dz = j(q = 0)$]. Thus one may get a hint about the bias in the

interlayer magnetic coupling by considering Eqs. (23) and (24) in the limit $q = 0$. The RKKY term is

$$j_{\text{RKKY}}(0) = V^4 D(\varepsilon_F) / E_h^2, \quad (37)$$

where $D(\varepsilon_F)$ is the density of states at the Fermi level. The superexchange term $j_S(0)$ does not have such a simple limit. For $q = 0$ it becomes

$$j_S(0) = V^4 \sum_{nk} [\varepsilon_F - \varepsilon_{nk} - E_h]^{-3}, \quad (38)$$

where the sum is over *unoccupied* states. The terms in this sum drop off quickly as ε_{nk} increases; *unless the density of unoccupied states is highly peaked near to the Fermi level, it will be small*. For a given number N of unoccupied orbitals per atom, $|j_S(0)|$ is bounded from above by the quantity

$$j_{S, \text{max}} = V^4 N / E_h^3. \quad (39)$$

This simple analysis gives us a clue that the *structure* of the density of states, with a peak above but near to the Fermi level ε_F , is a key factor in getting the antiferromagnetic bias, because this could increase $j_S(0)$ [Eq. (38)].

To confirm this, we added a Lorentzian-shaped peak to the free electron gas density of states (DOS),

$$D(\varepsilon) = \sqrt{\varepsilon} + \frac{\sqrt{\varepsilon_F}}{(\varepsilon/\varepsilon_F - b)^2 + c^2}, \quad (40)$$

where the position of the peak is at $\varepsilon = b\varepsilon_F$, and c adjusts height of the peak (small c correspond to a large peak). By fixing the position, e.g., $b = 1.1$, and increasing the height of the peak from $c = 0.9$ to 0.3 , we are able to increase the antiferromagnetic bias in the coupling, as shown in Fig. 16(a). For fixed position and height of the peak, e.g., $b = 1.1$ and $c = 0.3$, the smaller E_h is chosen, the larger is the antiferromagnetic bias, as shown in Fig. 16(b). This situation reproduces the results we find from calculations of the interlayer magnetic coupling in Fe/Cr/Fe(001) multilayered structures by using realistic

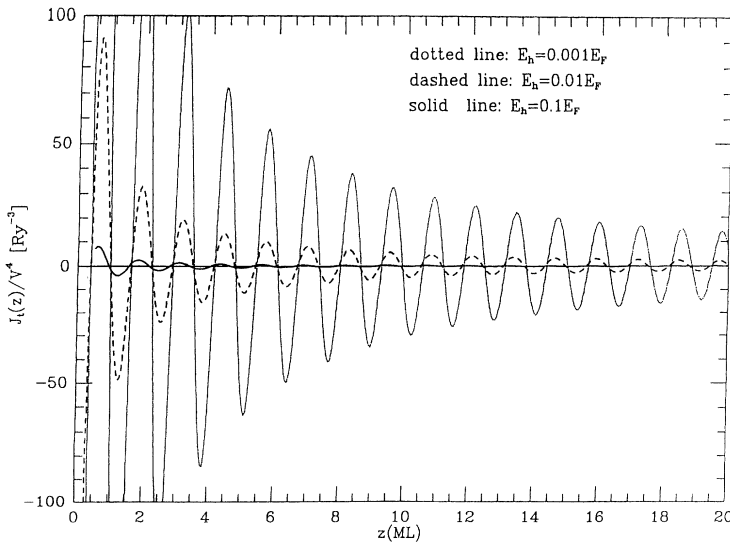


FIG. 15. The total interlayer magnetic coupling $J_t(z)$ in the free electron gas approximation calculated with $E_h = 0.001\varepsilon_F$, $0.01\varepsilon_F$, and $0.1\varepsilon_F$. There is no indication of a bias by changing E_h .

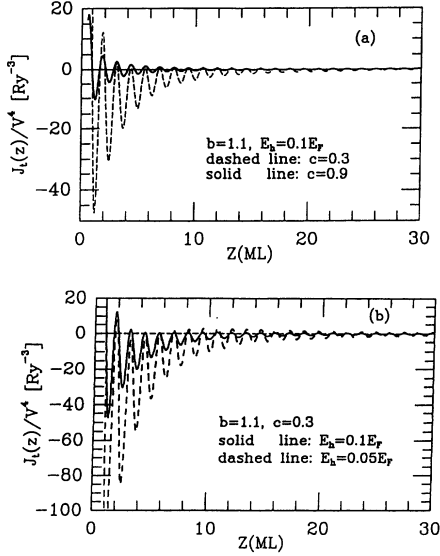


FIG. 16. The total interlayer magnetic coupling $J_t(z)$ when we have a peak in the density of states. (a) In both cases $b = 1.1$ and $E_h = 0.1\epsilon_F$: dashed line for $c = 0.3$ with large antiferromagnetic bias, and solid line for $c = 0.9$. (b) Calculated with $b = 1.1$ and $c = 0.3$, dashed line for $E_h = 0.05\epsilon_F$ with large antiferromagnetic bias, and solid line for $E_h = 0.1\epsilon_F$.

band structures.²⁵

The above calculation confirms a prediction by Fry *et al.*⁶⁴ for the criteria for the observation of oscillatory interlayer magnetic coupling with antiferromagnetic bias:

- (i) $D(\epsilon_F)$ should be a minimum.
- (ii) $D(\epsilon)$ should have peaks above but near to the Fermi level ϵ_F .

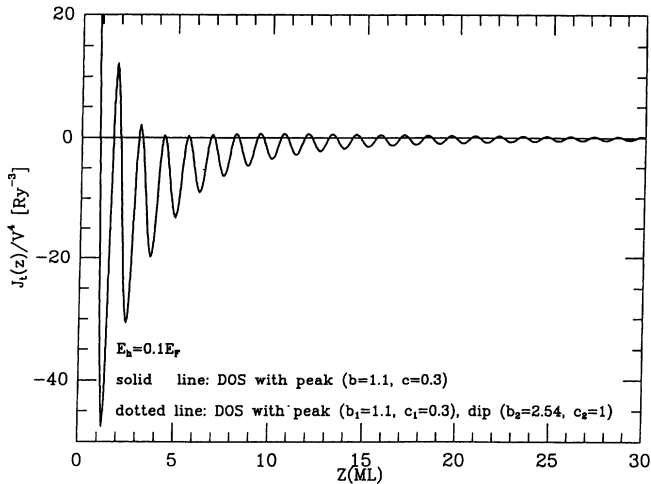


FIG. 17. Comparison of total coupling $J_t(z)$ calculated with $E_h = 0.1\epsilon_F$ for a density of states with a peak ($b = 1.1$, $c = 0.3$) (solid line), and with a peak ($b_1 = 1.1$ and $c_1 = 0.3$) and a dip ($b_2 = 2.54$ and $c_2 = 1$) so that the total number of states remains fixed (dotted line). They are almost equivalent to each other, and tiny difference can be seen only in small region of z .

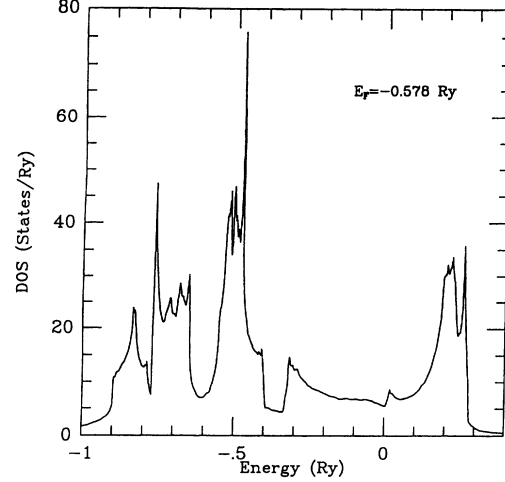


FIG. 18. Density of states for Cr from band structure calculation we used in our calculations.

- (iii) N/E_h should be large compared to $D(\epsilon_F)$.

One may call into question this conclusion because the number of states are not conserved for Eq. (40). In order to clarify this point, we subtract a Lorentzian-shaped peak, so as to keep the total number of states a constant. In this case, the density of states is written down as

$$D(\epsilon) = \sqrt{\epsilon} + \frac{\sqrt{\epsilon_F}}{(\epsilon/\epsilon_F - b_1)^2 + c_1^2} - \frac{\sqrt{\epsilon_F}}{(\epsilon/\epsilon_F - b_2)^2 + c_2^2}, \quad (41)$$

where b_1, c_1 and b_2, c_2 correspond to two different peaks. The relationship between these coefficients is

$$c_2[\pi/2 + \tan^{-1}(b_1/c_1)] = c_1[\pi/2 + \tan^{-1}(b_2/c_2)]. \quad (42)$$

When we use $b_1 = 1.1$, $c_1 = 0.3$, and $c_2 = 1.0$, we find $b_2 = 2.54$. The strongly antiferromagnetic bias in the interlayer magnetic coupling still remains, as shown in Fig. 17. It is almost equivalent to the one peak case and confirms the essential role of the peak in producing the antiferromagnetic bias.

We conclude that the antiferromagnetic bias arises from the structure in the density of states for the realistic band structure of Cr; see Fig. 18.

G. Antiferromagnetically coupled transition-metal structures

Using the criteria listed in the previous section, one can understand why Cr serves as an appropriate spacer layer to obtain antiferromagnetic coupling between Fe layers, and one can suggest other systems similar to Fe/Cr without detailed calculations of the coupling, Eq. (26). The well-known density of states of Cr (see Fig. 18) is characterized by a Fermi level that falls in a minimum between the e_g and t_{2g} peaks of the d -electron density of states.⁶⁵ The e_g peak just above the Fermi level satisfies

TABLE I. Band parameter for possible metals.^a

Metal	a (a.u.)	c (a.u.)	$D(E_F)$ (Ry/atom) ⁻¹	Probability
hcp				
Ti	5.58	8.85	8.1	High
Zr	6.11	9.73	7.9	High
Ru	5.11	8.09	11.5	High
Hf	6.04	9.56	6.7	High
Re	5.22	8.42	11.0	Medium
Os	5.17	8.16	9.5	High
bcc				
Cr	5.45	...	9.6	High
Mo	5.95	...	8.1	High
W	5.98	...	5.7	High
fcc				
Ir	7.26	...	12.7	Medium
Rh	7.18	...	18.7	Low

^a J. L. Fry *et al.*, J. Appl. Phys. **69**, 4780 (1991).

criterion (ii) and the Fe/Cr surface magnetic state with $E_h = 0.08$ Ry satisfies criterion (iii).

Table I gives a listing of the elements, lattice structure, and density of states $D(\varepsilon_F)$ for spacer materials that are likely to display antiferromagnetic coupling.⁶⁴ The column labeled “probability” is an estimate of how likely the elements are to satisfy the criteria of the previous subsection.

VI. DISCUSSION OF RESULTS

We have presented two types of mechanisms which excite a nominally nonmagnetic spacer layer sandwiched between magnetic layers to interpret the interlayer magnetic coupling in metallic multilayered structures: spin and virtual charge excitations. Spin excitations give rise to an RKKY-like coupling $[J_{\text{RKKY}}(z)]$, while virtual charge excitations produce superexchange coupling $[J_S(z)]$. This theoretical model implies that the spin polarization pattern in the spacer layer could be different from that of the interlayer magnetic coupling, a result which has some experimental support.⁴² Another characteristic of this model is that it predicts that some metallic multilayered structures can have relatively large antiferromagnetic biases of the interlayer magnetic coupling in the preasymptotic region, a result which is also in agreement with some recent experiments.^{4,42,66} Thus, the combination of both couplings gives a more complete understanding of the interlayer magnetic coupling in metallic multilayered structures.

As a first step, we have shown how the RKKY-like coupling alone cannot explain interlayer magnetic coupling in Fe/Cr/Fe(001) systems. In this context, we have calculated the spin polarization in a Cr layer deposited on an Fe substrate, and find it agrees reasonably well with experimental data. This spin polarization is picked up by an Fe *overlayer* to form an RKKY-like interlayer

magnetic coupling $[J_{\text{RKKY}}(z)]$; this coupling which has a ferromagnetic bias does not resemble experimental data which has an antiferromagnetic bias in Fe/Cr/Fe(001). Then we have demonstrated that the RKKY-like and superexchange couplings together give the antiferromagnetically biased coupling observed in Fe/Cr/Fe(001) systems [taken together they are equivalent to a conventional RKKY coupling in the free electron approximation that is produced by a structureless point contact potential, i.e., Eq. (1)]. The $J_{\text{RKKY}}(z)$ contains information of the Fermi surface of the spacer layers, e.g., the extremal wave vectors that span the Fermi surface which correspond to the short- and long-range oscillations. Therefore those calculations which limit themselves to J_{RKKY} miss the bias in the coupling, if there is one. In addition those calculation which do not include the correlations implied by our use of the Anderson *s-d* mixing interaction [see Eq. (17)], will also miss the superexchange contribution to the interlayer magnetic coupling.⁶⁷

The local levels of the transition-metal ions at the interface are not constants as we have initially assumed. The mixing interaction leads to a broadening or virtual bound state description of these levels; this introduces complex energy levels which we have been taken into account in our calculations. However, when considering a sheet of magnetic impurities, E_h (local states) represents a two-dimensional band of states. The dispersion of these states should be incorporated in future evaluations of the coupling by summing over E_h ; we have modeled this case by considering several values for E_h , and find that this dispersion in E_h does not alter the principal conclusions arrived at in this paper.

ACKNOWLEDGMENTS

This research was supported in part by the Research Challenge Fund of New York University, the Office of Naval Research Grant No. N00014-91-J-1695 (Z.-P.S.

and P.M.L.) and by the Robert A. Welch Foundation and the Texas Advanced Research Program (J.L.F.).

APPENDIX: SUSCEPTIBILITY AND INTERLAYER MAGNETIC COUPLING

In this appendix, we relate the susceptibility function of a spacer layer with the interlayer magnetic coupling in metallic multilayered structures.

The susceptibility function of a system is defined by its linear response to an external magnetic field:

$$\mathbf{m}(\mathbf{r}) = \int \chi(\mathbf{r}, \mathbf{r}') \mathbf{H}(\mathbf{r}') d\mathbf{r}' \quad (\text{A1})$$

or

$$\mathbf{m}_{\mathbf{q}} = \sum_{\mathbf{q}'} \chi_{\mathbf{q}\mathbf{q}'} \mathbf{h}_{\mathbf{q}'} \quad (\text{A2})$$

where $\mathbf{m}_{\mathbf{q}}$ and $\chi_{\mathbf{q}\mathbf{q}'}$ are the spatial Fourier transforms of $\mathbf{m}(\mathbf{r})$ and $\chi(\mathbf{r}, \mathbf{r}')$, respectively. If the system is homogeneous, one has a reduced version, $\chi_{\mathbf{q}\mathbf{q}'} = \chi_{\mathbf{q}} \delta_{\mathbf{q}\mathbf{q}'}$.

If we assume that the perturbation of the conduction electron gas is produced by magnetic impurities in a host metal, we can represent it by a field acting on the spin of the conduction electrons,

$$h_{\mathbf{q}} = A(\mathbf{q}) S_{\mathbf{q}} \quad (\text{A3})$$

where $A(\mathbf{q})$ represents an interaction between the spins of the local and conduction electrons as discussed in Sec. II, and

$$S_{\mathbf{q}} = \frac{1}{\sqrt{N}} \sum_n e^{i\mathbf{q} \cdot \mathbf{R}_n} S_n \quad (\text{A4})$$

Here S_n is an impurity spin on a lattice site \mathbf{R}_n , and N is the total number of impurities. Then the interaction energy between the induced magnetization and field, in the case of a homogeneous system, can be easily written down as

$$E_{\text{int}} = \sum_{\mathbf{q}} \chi_{\mathbf{q}} h_{\mathbf{q}}^2 \quad (\text{A5})$$

By placing Eq. (A4) in Eq. (A5) we find

$$E_{\text{int}} = \sum_{\mathbf{q}} A^2(\mathbf{q}) \chi(\mathbf{q}) \sum_{nn'} e^{i\mathbf{q} \cdot (\mathbf{R}_n - \mathbf{R}_{n'})} \mathbf{S}_n \cdot \mathbf{S}_{n'} \quad (\text{A6})$$

This contains self-energy corrections ($n = n'$); but the coupling energy comes from terms with $n \neq n'$ and is written as

$$E_{\text{coup}} = \sum_{\mathbf{q}} A^2(\mathbf{q}) \chi(\mathbf{q}) \sum_{n \neq n'} e^{i\mathbf{q} \cdot (\mathbf{R}_n - \mathbf{R}_{n'})} \mathbf{S}_n \cdot \mathbf{S}_{n'} \quad (\text{A7})$$

When $A(\mathbf{q})$ is taken as a constant then each mode is proportional to the susceptibility $\chi(\mathbf{q})$.

In deriving \mathbf{q} -dependent susceptibilities $\chi(\mathbf{q})$ one usually models the local-moment-conduction-electron spin

interaction by a Zeeman Hamiltonian

$$H_{\text{Zeeman}} = \sum_i \mathbf{s}_i \cdot \mathbf{h}_i \quad (\text{A8})$$

where \mathbf{s}_i is a spin density of the conduction electrons in a host, and \mathbf{h}_i is the magnetic field associated with the magnetic impurities. Then the interaction energy can be expressed as

$$\begin{aligned} I_{n_1 k, n_2 k'} &= \langle n_1 k \sigma | \sum_i \mathbf{s}_i \cdot \mathbf{h}_i | n_2 k' \sigma' \rangle \\ &= \sum_i \langle n_1 k \sigma | \mathbf{s}_i \cdot \mathbf{h}_i | n_2 k' \sigma' \rangle \end{aligned} \quad (\text{A9})$$

If one takes an extended source, e.g., a one-mode source

$$\mathbf{h}_i = \mathbf{h}_{\mathbf{q}} e^{i\mathbf{q} \cdot \mathbf{r}_i} \quad (\text{A10})$$

the interaction energy, Eq. (A9), becomes

$$\begin{aligned} I_{n_1 k, n_2 k'} &= \mathbf{h}_{\mathbf{q}} \cdot \sum_i \langle n_1 k \sigma | \mathbf{s}_i e^{i\mathbf{q} \cdot \mathbf{r}_i} | n_2 k' \sigma' \rangle \\ &= \mathbf{h}_{\mathbf{q}} \cdot \langle \sigma | \mathbf{s} | \sigma' \rangle \langle n_1 k | e^{i\mathbf{q} \cdot \mathbf{r}} | n_2 k' \rangle \end{aligned} \quad (\text{A11})$$

The matrix element $\langle n_1 k | e^{i\mathbf{q} \cdot \mathbf{r}} | n_2 k' \rangle$ in the above equation is defined as $M_{n_1 k, n_2 k'}^*(\mathbf{q})$ in Sec. II, and then one obtains the relationship

$$I_{n_1 k, n_2 k'} \sim M_{n_1 k, n_2 k'}^*(\mathbf{q}) \quad (\text{A12})$$

Equation (A12) gives a physical reason for making the ansatz $V_{n_1 k} V_{n_2 k'}^* = V^2 M_{n_1 k, n_2 k'}^*(\mathbf{q})$ we used in our calculations; see Secs. II C and IV A. To mimic local interactions this can only make sense if one does a sum over \mathbf{q} , because $M_{n_1 k, n_2 k'}(\mathbf{q})$ is definitively nonlocal.

If one takes a local source, e.g.,

$$\mathbf{h}_i = \mathbf{h} \delta(\mathbf{r}_i - \mathbf{R}) \quad (\text{A13})$$

which means that $\mathbf{h}_{\mathbf{q}} = \mathbf{h} e^{i\mathbf{q} \cdot \mathbf{R}}$ for all \mathbf{q} , the interaction energy, Eq. (A9), reduces to

$$\begin{aligned} I_{n_1 k, n_2 k'} &= \mathbf{h} \cdot \sum_i \langle n_1 k \sigma | \mathbf{s}_i \delta(\mathbf{r}_i - \mathbf{R}) | n_2 k' \sigma' \rangle \\ &= \mathbf{h} \cdot \langle \sigma | \mathbf{s} | \sigma' \rangle \langle n_1 k | \delta(\mathbf{r} - \mathbf{R}) | n_2 k' \rangle \end{aligned} \quad (\text{A14})$$

Generally, the state $|nk\rangle$ is a Bloch wave and has a form

$$|nk\rangle = e^{i\mathbf{k} \cdot \mathbf{r}} u_{\mathbf{k}}(\mathbf{r}) \quad (\text{A15})$$

where $u_{\mathbf{k}}(\mathbf{r})$ is a periodic function. Then the matrix elements in Eq. (A14) reduce to

$$\begin{aligned} \langle n_1 k | \delta(\mathbf{r} - \mathbf{R}) | n_2 k' \rangle &= e^{i(\mathbf{k}' - \mathbf{k}) \cdot \mathbf{R}} u_{\mathbf{k}}^*(\mathbf{R}) u_{\mathbf{k}'}(\mathbf{R}) \\ &= e^{i(\mathbf{k}' - \mathbf{k}) \cdot \mathbf{R}} u_{\mathbf{k}}^*(0) u_{\mathbf{k}'}(0) \end{aligned} \quad (\text{A16})$$

where \mathbf{R} is supposed to be a lattice site. Then for a local source we have

$$|I_{n_1 k, n_2 k'}|^2 \sim |u_{\mathbf{k}}(0)|^2 |u_{\mathbf{k}'}(0)|^2 \quad (\text{A17})$$

As $|u_{\mathbf{k}}(0)|^2$ is a slowly varying function of \mathbf{k} , one can take $|I_{n_1 k, n_2 k'}|^2 \approx \text{const}$, which corresponds to the ansatz $|V_{n_1 k}|^2 |V_{n_2 k'}|^2 = \text{const}$ we made for large \mathbf{q} ; see Secs. II C and IV A.

*Present address: Department of Physics, University of California at Davis, Davis, CA 95616.

¹S. S. P. Parkin, N. More, and K. P. Roche, Phys. Rev. Lett. **64**, 2304 (1990).

²J. Unguris, R. J. Celotta, and D. T. Pierce, Phys. Rev. Lett. **67**, 140 (1991).

³S. T. Purcell *et al.*, Phys. Rev. Lett. **67**, 903 (1991).

⁴S. Demokritov, J. A. Wolf, P. Grünberg, and W. Zinn, in

- Magnetic Surfaces, Thin Films, and Multilayers*, edited by S. S. P. Parkin, H. Hopster, J.-P. Renard, T. Shinjo, and W. Zinn, MRS Symposia Proceedings No. 231 (Materials Research Society, Pittsburgh, 1992), p. 133.
- ⁵S. T. Purcell, M. T. Johnson, N. W. E. McGee, R. Coehoorn, and W. Hoving, *Phys. Rev. B* **45**, 13064 (1992).
 - ⁶Z. Q. Qiu, J. Pearson, A. Berger, and S. D. Bader, *Phys. Rev. Lett.* **68**, 1398 (1992).
 - ⁷M. T. Johnson, S. T. Purcell, N. W. E. McGee, R. Coehoorn, J. aan de Stegge, and W. Hoving, *Phys. Rev. Lett.* **68**, 2688 (1992).
 - ⁸M. T. Johnson, R. Coehoorn, J. J. de Vries, N. W. E. McGee, J. aan de Stegge, and P. J. H. Bloemen, *Phys. Rev. Lett.* **69**, 969 (1992).
 - ⁹P. M. Levy, K. Ounandjela, S. Zhang, Y. Wang, C. B. Sommers, and A. Fert, *J. Appl. Phys.* **67**, 5914 (1991).
 - ¹⁰F. Herman, J. Sticht, and M. van Schilfgaarde, *J. Appl. Phys.* **69**, 4783 (1991); in *Magnetic Surfaces, Thin Films, and Multilayers* (Ref. 4), p. 195.
 - ¹¹H. Hasegawa, *Phys. Rev. B* **42**, 2368 (1990); **43**, 10803 (1991).
 - ¹²D. Stoeffler and F. Gautier, *Prog. Theor. Phys. Suppl.* **101**, 139 (1990); *Phys. Rev.* **44**, 10389 (1991); D. Stoeffler, K. Ounadjela, and F. Gautier, *J. Magn. Magn. Mater.* **93**, 386 (1991).
 - ¹³D. M. Edwards, J. Mathon, R. B. Muniz, and M. S. Phan, *J. Phys. Condens. Matter* **3**, 4941 (1991).
 - ¹⁴J. Barnas, *J. Magn. Magn. Mater.* **111**, L215 (1992).
 - ¹⁵R. P. Erickson, K. B. Hathaway, and J. R. Cullen, *Phys. Rev. B* **47**, 2626 (1993).
 - ¹⁶K. B. Hathaway and J. R. Cullen, *J. Magn. Magn. Mater.* **104-107**, 1840 (1991).
 - ¹⁷J. R. Cullen and K. B. Hathaway, *J. Appl. Phys.* **70**, 5879 (1991).
 - ¹⁸M. D. Stiles, *Phys. Rev. B* **48**, 7238 (1993).
 - ¹⁹N. W. Ashcroft and N. D. Mermin, *Solid State Physics* (Library of Congress Cataloging in Publication Data, Washington, D.C., 1976), pp. 306-307.
 - ²⁰M. A. Ruderman and C. Kittel, *Phys. Rev.* **96**, 99 (1954).
 - ²¹T. Kasuya, *Prog. Theor. Phys.* **16**, 45 (1956).
 - ²²K. Yosida, *Phys. Rev.* **106**, 893 (1957).
 - ²³P. Bruno and C. Chappert, *Phys. Rev. Lett.* **67**, 1602 (1991); **67**, 2592(E) (1991); *Phys. Rev. B* **46**, 261 (1992).
 - ²⁴L. M. Roth, H. J. Zeiger, and T. A. Kaplan, *Phys. Rev.* **149**, 519 (1966).
 - ²⁵Y. Wang, P. M. Levy, and J. F. Fry, *Phys. Rev. Lett.* **65**, 2732 (1990).
 - ²⁶D. M. Deaven, D. S. Rokhsar, and M. Johnson, *Phys. Rev. B* **44**, 5977 (1991).
 - ²⁷Z.-P. Shi, P. M. Levy, and J. L. Fry, *Phys. Rev. Lett.* **69**, 3678 (1992).
 - ²⁸Y. Yafet, *J. Appl. Phys.* **61**, 4058 (1987).
 - ²⁹S. H. Liu, R. P. Gupta, and S. K. Sinha, *Phys. Rev. B* **4**, 1100 (1971).
 - ³⁰Y. Yafet, *Phys. Rev. B* **36**, 3948 (1987).
 - ³¹W. Baltensperger and J. S. Helman, *Appl. Phys. Lett.* **57**, 2954 (1990).
 - ³²Z. Q. Qiu, J. Pearson, and S. D. Bader, *Phys. Rev. B* **46**, 8659 (1992).
 - ³³W. M. Fairbairn and S. Y. Yip, *J. Phys. Condens. Matter* **2**, 4197 (1990).
 - ³⁴R. E. Watson, A. J. Freeman, and S. Koide, *Phys. Rev.* **186**, 625 (1969).
 - ³⁵J. Callaway *et al.*, *Phys. Rev. B* **28**, 3818 (1983).
 - ³⁶Z.-P. Shi, P. M. Levy, and J. L. Fry, *J. Appl. Phys.* **73**, 5975 (1993).
 - ³⁷K. Schwartzman, J. L. Fry, and Y. Z. Zhao, *Phys. Rev. B* **40**, 454 (1989).
 - ³⁸P. W. Anderson, *Phys. Rev.* **124**, 24 (1961).
 - ³⁹J. R. Schrieffer and P. A. Wolff, *Phys. Rev.* **149**, 491 (1966).
 - ⁴⁰J. Friedel, *Nuovo Cimento Suppl.* **7**, 287 (1958).
 - ⁴¹T. G. Walker, A. W. Pang, H. Hopster, and S. F. Alvarado, *Phys. Rev. Lett.* **69**, 1121 (1992).
 - ⁴²J. Unguris, R. J. Celotta, and D. T. Pierce, *Phys. Rev. Lett.* **69**, 1125 (1992).
 - ⁴³D. G. Laurent, J. Callaway, J. L. Fry, and N. E. Brener, *Phys. Rev. B* **23**, 4977 (1981).
 - ⁴⁴E. Fawcett, *Rev. Mod. Phys.* **60**, 209 (1988).
 - ⁴⁵B. Caroli, *J. Phys. Chem. Solids* **28**, 1427 (1967).
 - ⁴⁶Q. Zhang and P. M. Levy, *Phys. Rev. B* **34**, 1884 (1986).
 - ⁴⁷C. E. T. Goncalves da Silva and L. M. Falicov, *J. Phys. C* **5**, 63 (1972).
 - ⁴⁸V. I. Anisimov *et al.*, *Phys. Rev. B* **37**, 5598 (1988); V. P. Antropov *et al.*, *ibid.* **37**, 5603 (1988).
 - ⁴⁹C. Proetto and A. López, *Phys. Rev. B* **25**, 7037 (1982).
 - ⁵⁰C. Chappert and J. P. Renard, *Europhys. Lett.* **15**, 553 (1991).
 - ⁵¹R. Coehoorn, *Phys. Rev. B* **44**, 9331 (1991).
 - ⁵²B. Dreyfus, R. Maynard, and A. Quattropani, *Phys. Rev. Lett.* **13**, 342 (1964).
 - ⁵³A. Bardasis *et al.*, *Phys. Rev. Lett.* **14**, 298 (1965).
 - ⁵⁴K. Yosida and A. Okiji, *Phys. Rev. Lett.* **14**, 301 (1965).
 - ⁵⁵J. C. Slonczewski, *Phys. Rev. Lett.* **67**, 3172 (1991).
 - ⁵⁶M. Rühlig, R. Schfer, A. Hubert, R. Mosler, J. A. Wolf, S. Demokritov, and P. Grünberg, *Phys. Status Solidi A* **125**, 635 (1991).
 - ⁵⁷B. Heinrich *et al.*, *Phys. Rev. B* **44**, 9348 (1991).
 - ⁵⁸P. A. Wolff, *Phys. Rev.* **120**, 814 (1960).
 - ⁵⁹K. Schwartzman and J. L. Fry, *J. Phys. Condens. Matter* **2**, 9085 (1990); K. Schwartzman, E. J. Hartford, and J. L. Fry, *J. Appl. Phys.* **67**, 4552 (1990).
 - ⁶⁰J. Callaway and A. K. Chatterjee, *J. Phys. F* **8**, 2569 (1978).
 - ⁶¹R. P. Gupta and S. K. Sinha, *Phys. Rev. B* **3**, 2401 (1971).
 - ⁶²R. E. Watson and A. J. Freeman, *Phys. Rev.* **152**, 566 (1966).
 - ⁶³B. Giovannini, M. Peter, and J. R. Schrieffer, *Phys. Rev. Lett.* **12**, 736 (1964).
 - ⁶⁴J. L. Fry, E. C. Ethridge, P. M. Levy, and Y. Wang, *J. Appl. Phys.* **69**, 4780 (1991).
 - ⁶⁵D. A. Papaconstantopoulos, *Handbook of the Band Structure of Elemental Solids* (Plenum, New York, 1986).
 - ⁶⁶B. Heinrich *et al.*, in *Magnetic Ultrathin Films: Multilayers and Surfaces, Interfaces and Characterizations*, edited by B. T. Jonker *et al.*, MRS Symposia Proceedings No. 313 (Materials Research Society, San Francisco, 1993), p. 119.
 - ⁶⁷M. van Schilfgaarde and F. Herman, *Phys. Rev. Lett.* **71**, 1923 (1993). They have made a first-principles calculation and have used a local spin density approximation to calculate the interlayer magnetic coupling in Fe/Cr. While they are able to find the oscillations they do not find evidence for a bias in the coupling.